T-4318

SORPTION OF THORIUM AT THE HEMATITE/WATER INTERFACE IN THE PRESENCE OF MARINE COLLOIDAL MATERIAL

by

Kathleen M. Rosow

A thesis submitted to the Faculty and Board of Trustees of the Colorado School of Mines in partial fulfillment of the requirements for the degree of Master of Science (Environmental Science and Engineering).

Golden, Colorado

Date 4/1/94

Signed: Kathleen M. Rosow

Approved: Bruce D. Honeyman
Thesis Advisor

Golden, Colorado

Date 4/1/94

John Cordes
Division Chair
Environmental Science and Engineering

ABSTRACT

Thorium isotopes have long been used by oceanographers to gain insights into the dynamics of marine particles as well as the characteristics of elements scavenged by sinking particles through sorptive processes. Recent studies of thorium behavior point to the role of colloidal material (i.e., 1000 D - 0.4μm) as an important component in thorium geochemistry. In this study, the effect of marine colloidal organic matter (COM) on the adsorption of thorium by hematite (a metal oxide) was examined as a function of pH and ionic strength. Th(IV) is an extremely surface-active radionuclide and sorbs onto hematite as an inner-sphere complex in the absence of competing ligands. In the presence of COM, which sorbs onto hematite in a ligand-like manner, Th(IV) sorption is enhanced at low pH's. In contrast, COM sorption onto hematite is unaffected by Th(IV), at the COM/Th(IV) ratios studied. Th(IV) and COM sorption onto hematite is independent of ionic strength (I) for 0.01 M < I < 0.1 M $NaClO_4$, as is Th(IV) sorption onto hematite in the presence of COM. Data are modeled using the Triple-Layer Model of Davis *et al.*, (1978).

TABLE OF CONTENTS

LIST OF FIGURES

LIST OF TABLES

ACKNOWLEDGMENTS

I would like to extend my appreciation to Dr. Bruce Honeyman for his advice and direction throughout this thesis research project, and to Dr.'s Linda Figueroa and Ron Klusman for their added support. I acknowledge the NSF Ocean Sciences (OCE - 9012103) and DOE Coastal Margins Program (92ER61421) for project funding. A special thanks to Dr. Peter Santschi, Laudong Guo, and Matt Quigley (Texas A & M University) for providing the colloidal material, thorium and carbon analysis, and to Bob Klug and Bob McGrew (Metallurgy, CSM) for taking the scanning electron micrograph (SEM) photographs of the hematite particles. My graduate student officemates, Denise Delozier, Holly Hutton and Peter Stout, proved to be an inexhaustible source of laughter relief throughout the project, and my husband, Tim Murphy, provided me with constitutional support and reality checks when needed.

Chapter 1

INTRODUCTION

The understanding and interpretation of the marine chemistry of thorium [Th(IV)] by oceanographers has changed significantly over the last four decades. Box model descriptions (e.g., Bhat, 1969; Broecker *et al.,* 1973) of Th(IV) scavenging by particles sufficiently large to sink has led to the awareness that Th(IV) isotopes can be used to trace submicron particles and components of the carbon cycle (Baskaran, *et al.*, 1992; Honeyman and Santschi, 1992; Moran and Buessler, 1993). Thorium isotopes are no longer considered to sorb to all particles equally; rather, it has been realized that Th(IV) partitions between ligands in response to their chemical identity and concentration. This understanding has led to the hypothesis that thorium is likely distributed throughout the particle pools by coupled physical, chemical and biological processes. The purpose of this thesis is to understand the role of marine colloidal organic material (COM) on the surface activity of Th(IV).

1.1 Purpose and organization of thesis

This thesis contains the results of a laboratory study on the partitioning of thorium [Th(IV)] between solid and solution phases in simple electrolytes. The main objectives of this study were to examine Th(IV) adsorption in hematite (α-Fe_2O_3) suspensions using surface complexation modeling techniques, and to investigate the effect of marine colloidal organic matter (COM) on Th(IV) adsorption. The approach taken in this study was to understand adsorption of Th(IV) in ternary systems (Th(IV)/hematite/COM) through examination of individual component processes: 1) Th(IV) adsorption by hematite, 2) COM adsorption by hematite, and 3) Th(IV) complexation with COM (Figure 1.1). In otherwords, is the whole the sum of its component parts? The results of this study broadens our basic understanding of the role of Th(IV) organic complexes in Th(IV) adsorption and scavenging in the marine water column. These results will ultimately be used together with field research and modeling work to provide a better understanding of the marine carbon cycle.

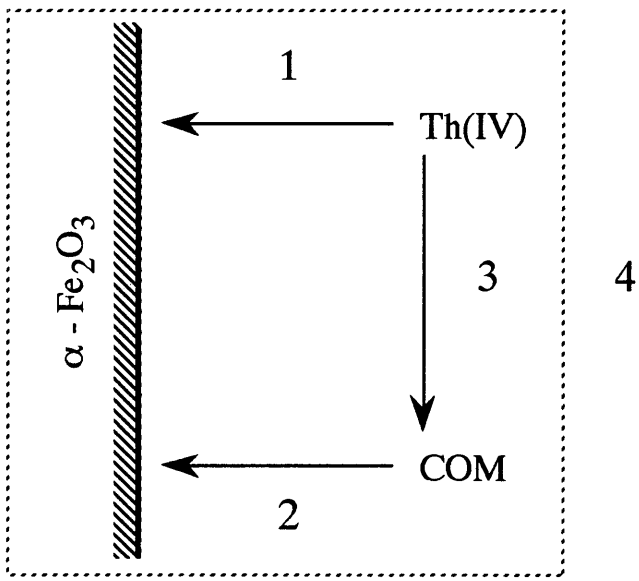

Figure 1.1 Research approach: interactions 1 - 3 represent individual component processes; interaction 4 represents Th(IV) sorption the ternary system.

This chapter contains an introduction to Th(IV) and colloidal organic matter (COM) including the concept of colloidal pumping. Chapter 2 contains background on surface complexation theory and the Triple-Layer Model, previous adsorption studies, and includes solution phase and surface reactions for the system. The materials and methods used in this study are described in Chapter 3. Experimental and modeling results are given in Chapter 4. The concluding chapter, Chapter 5, summarizes the results of this study.

1.2 Thorium: a surface active element

Thorium (IV), a highly surface reactive element of the actinide series, is present in both marine and terrestrial aqueous environments. It is found in nature as a tetravalent cation. Th(IV) has a limited solubility, although there is considerable range in the reported K_{sp} values (K_{sp} $Th(OH)_4 = 10^{-46.6}$ to $10^{-7.9}$, Baes and Mesmer, 1976; Niven, 1989). Three isotopes of thorium are generated within the sea by radioactive decay of more soluble parent nuclides (Figure 1.2): ^{230}Th (half-life 75,000 yr) is produced from the decay of ^{234}U, ^{234}Th (half-life 24 days) is produced from the decay of ^{238}U, and ^{228}Th (half-life 1.9 yr) is produced from the decay of ^{228}Ra (Broecker *et al.,* 1973). In addition, ^{232}Th is a primordial radionuclide (half-life 1.4×10^{10} yr). These radiogenic isotopes are particularly amenable to oceanic removal rate determinations because their decay rates and *in situ* production rates are well known. Removal rate determinations indicate that thorium has oceanic residence times of less than one year in surface water and less than 100 years in deep water (Broecker *et al.,* 1973; Bhat *et al.,* 1969; Moore and Sackett, 1964; Moore, 1969). While specific residence times depend on a number of factors including the nature of the particular thorium isotope, distance from the coast, and particle concentration, these relatively short residence times attest to the reactivity of thorium isotopes, in general.

Laboratory studies of thorium geochemistry have benefited from the high specific activity of the ^{234}Th isotope (half-life: 24.1 days). The high specific activity allows ^{234}Th quantification at low molar concentrations by liquid scintillation counting of its β-decay or analysis of the 64 kev gamma emission, and is beneficial for two reasons: 1) laboratory studies can use ^{234}Th concentrations similar to those found in nature (10^{-15} to 10^{-16} M), and 2) the use of low molar concentrations avoids exceeding solubility limits.

Thorium forms strong complexes with a variety of inorganic and organic ligands such as $H_2PO_4^-$, SO_4^{2-}, F^-, HPO_4^{2-} and OH^-, oxalate, citrate and EDTA (Langmuir and Herman, 1980). The ability of thorium to form these strong complexes with ligands present in natural waters suggests that Th(IV) may be more soluble than anticipated from hydroxide solubility calculations. Such determinations are critical because our ability to use thorium isotopes to predict the fate and transport of other reactive elements and particles in oceanic systems (Broecker *et al.,* 1973; Nozaki *et al.,* 1981; Santschi *et al.*, 1980) depends on our understanding of Th(IV) surface chemistry.

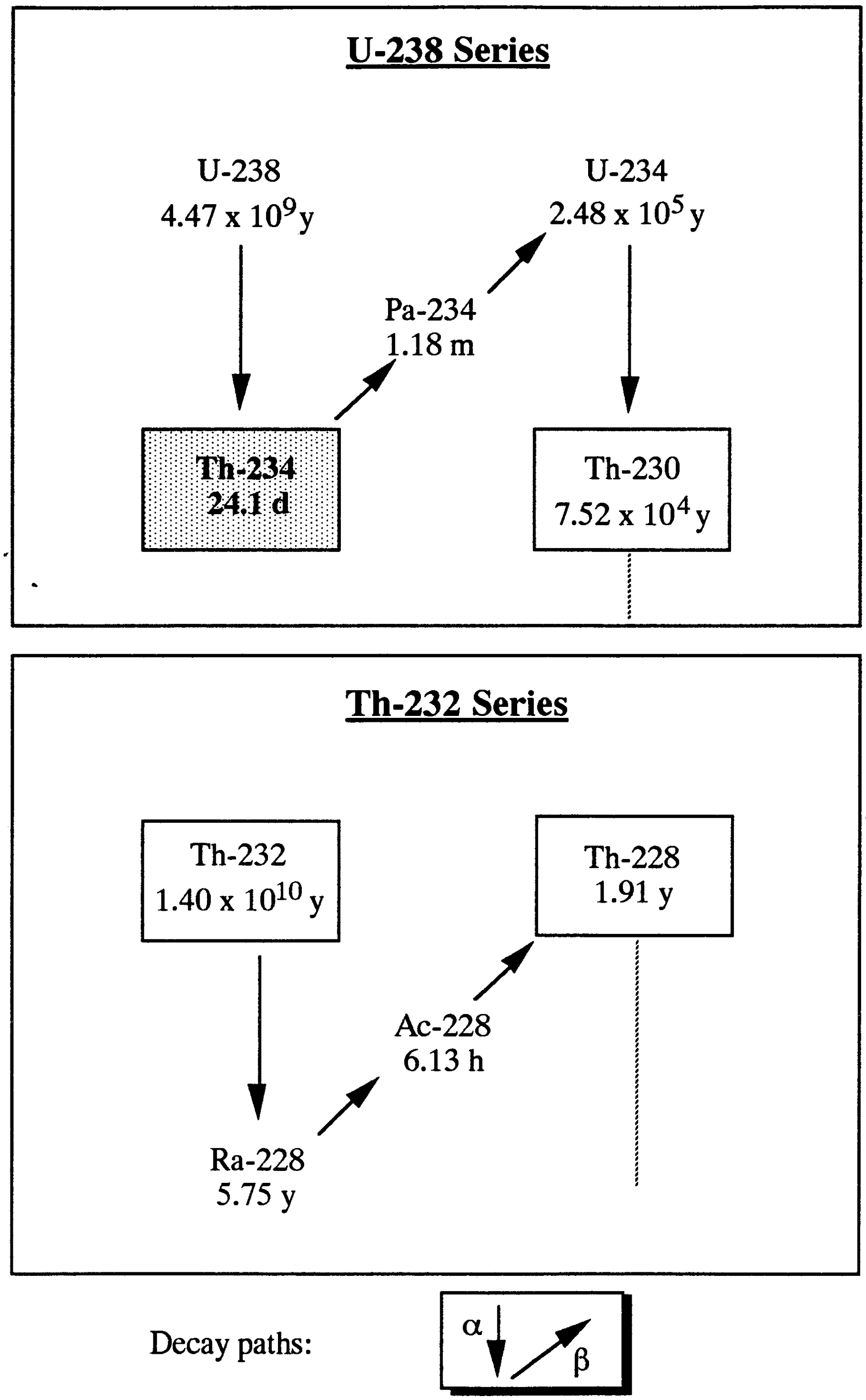

Figure 1.2 A portion of the natural uranium and thorium decay series (from Niven, 1989).

1.3 Marine colloidal organic matter

As oceanic particulate matter sinks, trace metals and other substances associated with these particles are removed from the water column. This removal by association with sinking particles is generally referred to as "scavenging" (Goldberg, 1954). The rate at which scavenging occurs is a requisite parameter in determining oceanic residence times for surface-active solutes such as thorium. Many attempts have been made to determine the quantity and distribution of particulate matter in the ocean to better understand its role in the ocean biogeochemical cycle. For example, Koike *et al.* (1990) examined the vertical distribution of submicron particles (0.38 - 1.0 μm) in the northern North Pacific Ocean. They found particle concentrations of 5 to 8 x 10^7 mL^{-1} in the top 40 meters, decreasing to 2 x 10^6 mL^{-1} at depths of 200 meters. Longhurst *et al.* (1992) found similar concentrations (10^7 mL^{-1}) of submicron particles (0.4 - 1.0 μm) in northwest Atlantic shelf water. These studies illustrate the shear magnitude of the submicron particle pool present in the oceanic water column. However, the particle size typically examined in these studies ranges from *ca.* 0.22 μm to 1.0 μm. This operational definition of particulate non-aqueous phase matter leaves material less than 0.22 μm in size, namely colloids, as constituents of the dissolved phase. The implications of colloidal organic matter (COM) as a component of the dissolved organic carbon (DOC) pool has only recently been addressed.

The oceanic water column carbon reservoir has three pools: (1) macro-particles, (2) colloidal organic matter, and (3) truly dissolved organic carbon (Honeyman and Santschi 1992). The term "colloid" is defined operationally and typically includes those particles from 1000 Daltons to 0.4 μm. Marine colloid chemical characteristics are poorly known due to its heterogeneous nature; for example, colloidal material can include constituents such as organic macromolecules, mineral fragments and condensation nuclei. Honeyman and Santschi (1989) proposed that the oceanic colloidal pool is of significance for two reasons. First, due to its heterogeneous composition, colloidal material has a large variety and number of chemical functional groups and generally a high capacity to complex trace elements. Second, these extremely small particles behave differently in the oceanic water column than their larger particle counterparts, which has implications regarding the fate of colloid-associated solutes compared to that of solutes associated with larger particles. An example of this dissimilar behavior is a study (Wells and Goldberg, 1991) that examined the quantity and vertical distribution of colloid particles (5 - 120 nm) off the coast of Santa Monica, California. They found the vertical profile to be highly stratified with particle numbers ranging from $<10^4$ particles mL^{-1} near the surface and at intermediate depths, to $> 10^9$ particles mL^{-1} near the lower thermocline (40 - 100 meters) and in bottom waters. Both the observed abundance and vertical distribution of these colloid particles differ substantially from that reported for the larger submicron particle pool.

It was previously considered that as submicron (colloidal) particles had insignificant settling rates in natural waters, they were unimportant in the downward flux of particles (Koike *et al.*, 1990). The corollary is that substances associated with these colloids do not leave the water column at an appreciable rate. More recently however, Honeyman and Santschi (1989) proposed that "colloidal pumping", the transfer of dissolved species to larger particles via colloidal intermediates, can facilitate the transfer of reactive substances (either dissolved or colloid-bound) to the sinkable particle pool. In this process, several interactions can occur: a) particle-reactive elements associate with particle surfaces, b) small particles aggregate with each other forming larger particles and, c) small particles aggregate with pre-existing large particles or aggregates (Figure 1.3). This model suggests that the vertical flux of trace metals and other reactive substances is controlled by small/large particle interactions. This colloidal pumping model was subsequently tested with measurements of the coagulation and sedimentation of uniformly spherical, ^{59}Fe labeled hematite particles in the presence of radioactive metals (Honeyman and Santschi, 1991). These laboratory studies show a shift in the distribution of hematite mass from filter-passing to filter-retained fractions as coagulation of the small particles into larger particles occurred, and movement of particle-associated trace elements into the larger particle-size pool during the process. These results demonstrate that solutes complexed to colloidal size particles having insignificant settling rates can move up the particle size spectrum by particle coagulation, and eventually be scavenged from the water column as these larger particles sink. The colloidal pumping model was also verified in natural systems (Santschi and Honeyman, 1991) by successfully predicting observed particle flux in three different marine environments.

Thorium transport in marine systems is a complicated process. A thorough understanding of the factors influencing thorium partitioning between solution and particulate phases is required before thorium transport as a whole can be understood.

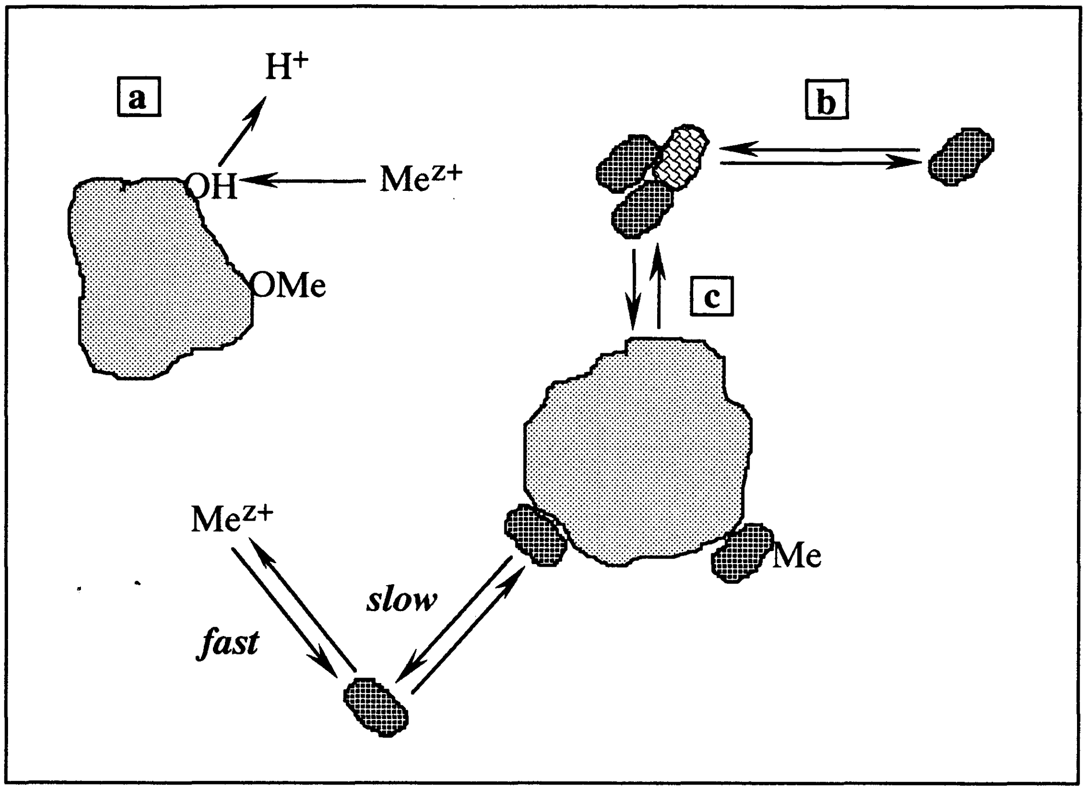

Figure 1.3 Schematic of colloidal pumping model (adapted from Honeyman, 1991).

One such factor to understand is the effect of submicron material (colloids) on thorium partitioning to suspended and settling particulate matter in the oceanic water column. Knowledge of this interaction will facilitate our understanding of the role of Th(IV) organic complexes in Th(IV) adsorption and scavenging in the marine water column.

Chapter 2

BACKGROUND

The process primarily responsible for the oceanic scavenging of many trace metals is adsorption (surface complexation). In the adsorption process, dissolved chemical species (solutes or sorbates) become associated with a surface (sorbent) by means of chemical reactions with surface functional groups (Davis and Kent, 1990; Dzombak and Morel, 1990). The observed solute adsorption by particles in the oceanic water column is the result of a number of competing reactions. These reactions include: 1) surface reactions such as protolysis and electrolyte exchange, 2) solution-phase reactions, such as hydrolysis and complexation, that may or may not involve the metal ion, and 3) other surface reactions involving the metal ion, hydrolysis species, and/or species that compete against the metal ion for surface sites (Honeyman, 1991). The following sections are intended to provide a general background on these reactions and how they are involved in surface complexation, summarize previous adsorption research, and provide the specific reactions for our experimental system.

2.1 Surface complexation theory and the Triple-Layer Model

The reactions describing overall adsorption in a particular system include protolysis and exchange reactions on the surface, solution phase reactions, and solute-surface reactions. A graphic illustrating these three aspects of adsorption is provided in Figure 2.1. Surface reactions such as surface protolysis and electrolyte exchange influence the physical, chemical and electrical properties a surface exhibits. These reactions involve the interaction of protons and background electrolytes with surface functional groups. Typical functional groups are hydroxyl moieties for metal oxides (Schindler and Stumm, 1987), whereas humic and fulvic acid functional groups characteristically include carboxylic and phenolic hydroxyls, and amines (Gamble, 1970; Choppin and Kullberg, 1978; Weber Jr.

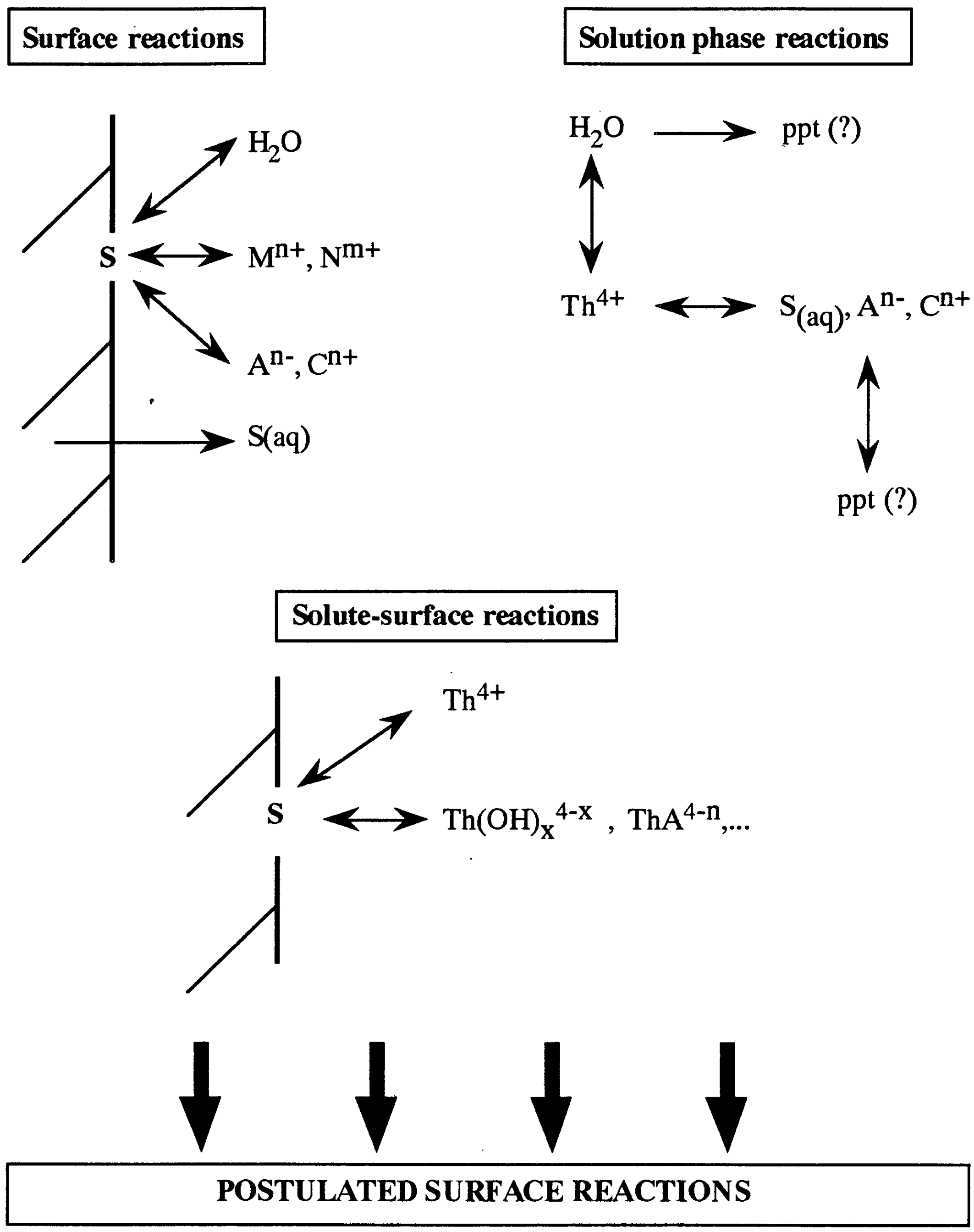

Figure 2.1 Reactions describing overall adsorption. Interactions: H_20 = hydrolysis or protolysis, M^{n+} and N^{m+} = metal ions; A^{n-} and C^{n+} = electrolytes; $S_{(aq)}$ = solubilization; ppt = solid phase formation (after Kent *et al.*, 1986).

et al., 1991). Protonation and deprotonation of these hydroxyl groups on metal oxides causes the surface to exhibit amphoteric behavior in water. This behavior is commonly described by analogy with diprotic acid dissociation in solution, where SO^-, SOH and SOH_2^+ represent a deprotonated, neutral and protonated surface, respectively. e.g.:

$$SOH_2^+ \overset{K_{a,1}}{=} SOH + H^+ \quad 2\text{-}1$$

$$SOH \overset{K_{a,2}}{=} H^+ + SO^- \quad 2\text{-}2$$

The ability of the surface hydroxyl groups to accept and release protons results in a surface charge that varies with pH. Surface charge is also influenced by the interaction of background electrolyte ions with these ionizable surface sites (Davis *et al.*, 1978). This is illustrated by the following reactions where A^- and C^+ represent an anion and cation, respectively, and the notation indicates that electrolyte ions are associated with surface sites as ion pairs:

$$SOH + C^+ = SO^- - C^+ + H^+ \quad 2\text{-}3$$

$$SOH + A^- + H^+ = SOH_2^+ - A^- \quad 2\text{-}4$$

Surface charge influences the distribution of ions in bulk solution and causes an accumulation of counterions along the surface interface. The concentration of these ions is greatest at the surface and falls off with increasing distance from the surface such that the net interfacial charge is zero and electroneutrality is maintained. This distribution has classically been described (Gouy-Chapman model) as an electrical double layer where two layers of charge exist: an inner layer which can include specifically adsorbed ions, and an outer layer containing all nonspecifically adsorbed counterions (Dzombak and Morel, 1990). This model of the diffuse double layer was subsequently refined (Stern-Graham model) to account for the finite size of ions which limits the inner boundary of the diffuse layer (Shaw, 1991). In the Stern-Graham model, an additional layer of charge exists (the Stern layer) which consists of specifically adsorbed counterions that can only approach the surface within some finite distance, likely the ionic radii of anions and the hydrated radii of cations (Davis and Kent, 1990). The surface charge (o plane) is now balanced by the charge in the Stern layer (β plane) plus that of the outer, diffuse layer. An illustration of this relationship is presented in Figure 2.2.

Solution phase reactions, such as hydrolysis and complex formation, control the solution species available for surface complexation. Hydrolysis of metal ions in aqueous solution can be viewed as the progressive replacement of coordinated water molecules by hydroxide groups. The number of hydrolyzed metal species formed depends primarily on the valence of the metal ion and solution pH. Solution-phase complex formation occurs similarly except that a ligand in solution, e.g. Cl^-, F^-, NH_3 and CN^-, complexes with the metal ion instead of a hydroxide group. These interactions are illustrated by the following general reactions, where Me^{z+} represents a trace metal and L^{n-} a ligand in solution:

solute hydrolysis: $$Me^{z+} + H_2O = MeOH^{(z-1)} + H^+ \quad \text{2-5}$$

complex formation: $$Me^{z+} + L^{n-} = MeL^{(z-n)} \quad \text{2-6}$$

The theories of solution coordination chemistry have been extended to solute-surface interactions such that the formation of solute-surface complexes is considered to be analogous to solute hydrolysis or complex formation in solution. This is demonstrated with the following equations where SOH, Me^{z+}, L^{n-} have their usual meanings:

$$SOH + Me^{z+} = SOMe^{(z-1)} + H^+ \quad \text{2-7}$$

$$SOH + Me^{z+} + H_2O = SOMeOH^{(z-1)} + 2H^+ \quad \text{2-8}$$

$$SOH + L^{n-} + H^+ = SOH_2^{+}\text{-}L^{(n-)} \quad \text{2-9}$$

$$SOH + MeL^{(z-n)} = SO^{-}\text{-}MeL^{(z-n)} + H^+ \quad \text{2-10}$$

$$SOH + MeL^{(z-n)} + H^+ = SOH_2^{+}\text{-}MeL^{(z-n)} \quad \text{2-11}$$

Note that reactions 2-9 through 2-11 are written as ion-pair complexes.

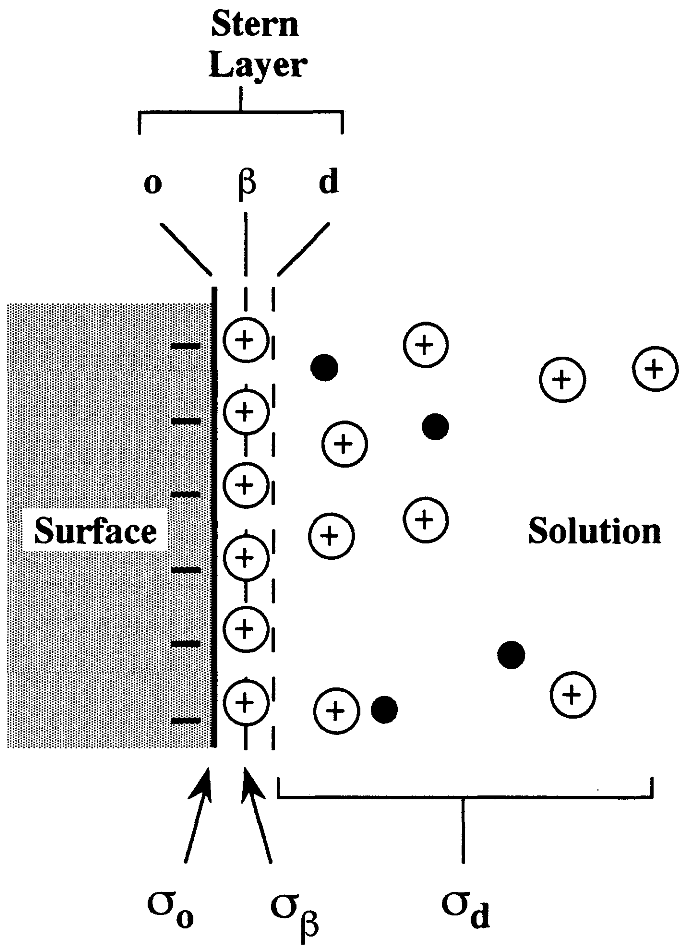

Figure 2.2 Schematic illustration of electrical double layer in Stern-Graham model - net interfacial charge is zero, i.e., $\sigma_o + \sigma_\beta + \sigma_d = 0$ (after Davis and Kent, 1990).

Figure 2.3 is a generalized illustration of the interactions that can occur in a heterogeneous system containing a mixture of solute complexing ligands. This schematic demonstrates that solutes can interact directly with either the surface or ligands in solution. Solute-ligand complexes can interact directly with the surface, but also have the capacity to remain in solution, thereby reducing the free solute concentration over that of a ligand-free system. (Benjamin and Leckie, 1981).

Solute adsorption is characteristically pH dependent and can be described as "metal-like" or "ligand-like" in behavior (Benjamin and Leckie, 1981). Metal-like adsorption exhibits an increase in adsorption with increasing pH, whereas ligand-like adsorption exhibits decreased sorption with increasing pH. The region of the adsorption curve that exhibits a rapid change in adsorption with pH is termed the "sorption edge". Metal-ligand complexes can exhibit either "metal-like" or "ligand-like" sorption behavior depending on what components are in the system.

A number of surface complexation models (SCM) exist that describe the equilibria between solution species (solutes) and surface complexes. All SCM's include the following principles (Davis and Kent, 1990):

1) The surface is composed of functional groups which react with solution species to form surface complexes. These surface complexes may be coordinative or ion pairs.

2) The reactions between surface functional groups and dissolved species can be described using mass-action expressions. Corrections are included to account for the work required to bring a charged species from bulk solution to a sorption plane of some net charge.

3) Surface charge and potential are the consequence of chemical reactions of the surface functional groups. They are secondary effects that result from surface coordination reactions.

4) The apparent binding constants determined for the mass-action expressions are surface empirical parameters related to thermodynamic constants via the rational activity coefficients of species [Sposito, 1983].

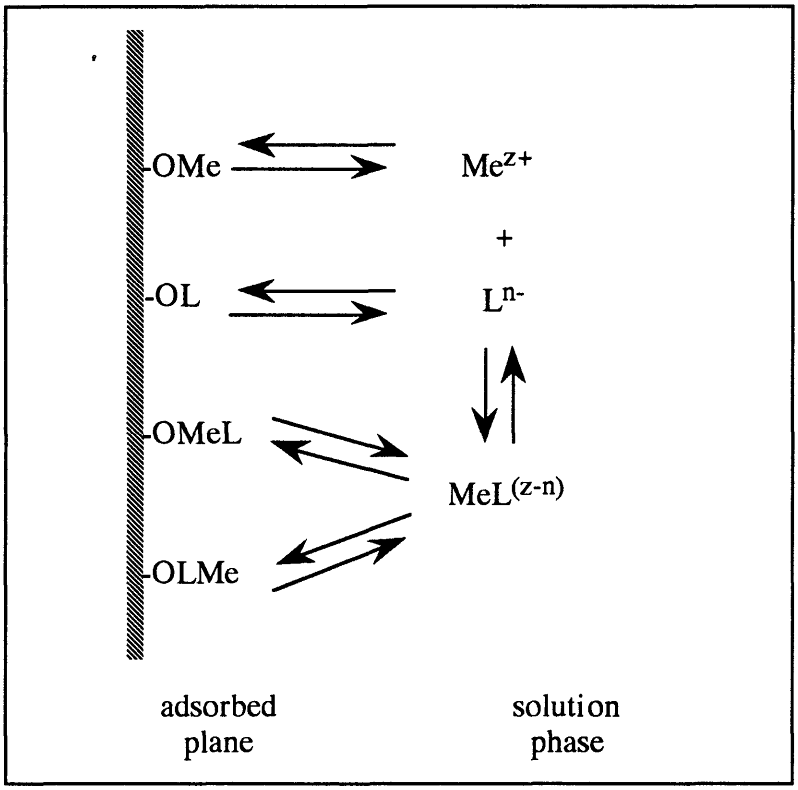

Figure 2.3 Possible metal-ligand-surface interactions in a ternary system (from Benjamin and Leckie, 1981). Me^{z+}, L^{n-}, and $MeL^{(z-n)}$ represent metal, ligand and metal-ligand complexes, respectively.

While sharing these basic tenets, SCM's differ in how they represent the sorbent interfacial structure, in otherwords, the number of planes and the charge-potential relationships associated with each model (Papelis *et al.*, 1988). The Triple-Layer Model (TLM) (1978) was used in our modeling efforts. This model assumes that three planes of attraction exist at the particle/solution interface (Figure 2.4): the σ_o *plane* (inner sphere) is an inner layer of surface hydroxyl groups that undergo proton exchange, the σ_β *plane* (outer sphere) is a compact layer of specifically adsorbed ions, and the σ_d *plane* is a diffuse layer of non-specifically adsorbed ions. Protons and strongly binding ions can be placed in the o - plane (coordination complexes), and weakly binding and electrolyte ions can be placed in the β -plane (ion pair formation). The assignment of cations and anions to the o- or β -plane depends on the effect of ionic strength on their sorption. Sorption that is insensitive to changes in ionic strength is considered to indicate o-plane or inner sphere complex formation (Hayes and Leckie, 1987; Hayes *et al.*, 1988), whereas, sorption that is affected by changes in ionic strength indicates β -plane or outer-sphere complex formation.

The relationship between charge (σ) and potential (ψ) for the Triple-Layer Model is:

$$\psi_o - \psi_\beta = \sigma_o / C_1$$

and

$$\psi_\beta - \psi_d = \sigma_o + \sigma_\beta / C_2$$

where C_1 and C_2 are the capacitances between the o- and β-planes and β- and d-planes, respectively. The parameters required for application of the TLM model include: sorbent specific surface area, site density, the inner and outer sphere capacitances (C_1 and C_2) and the equilibrium constants for all reactions taking place both in solution and at the surface (Hunter *et al.*, 1988).

2.2 Previous adsorption studies

Thorium adsorption in natural and laboratory systems has only been studied in the last 15 years or so. In natural oceanic systems, Th(IV) adsorption has been examined primarily by evaluating the association of Th(IV) with various particle size fractions in the

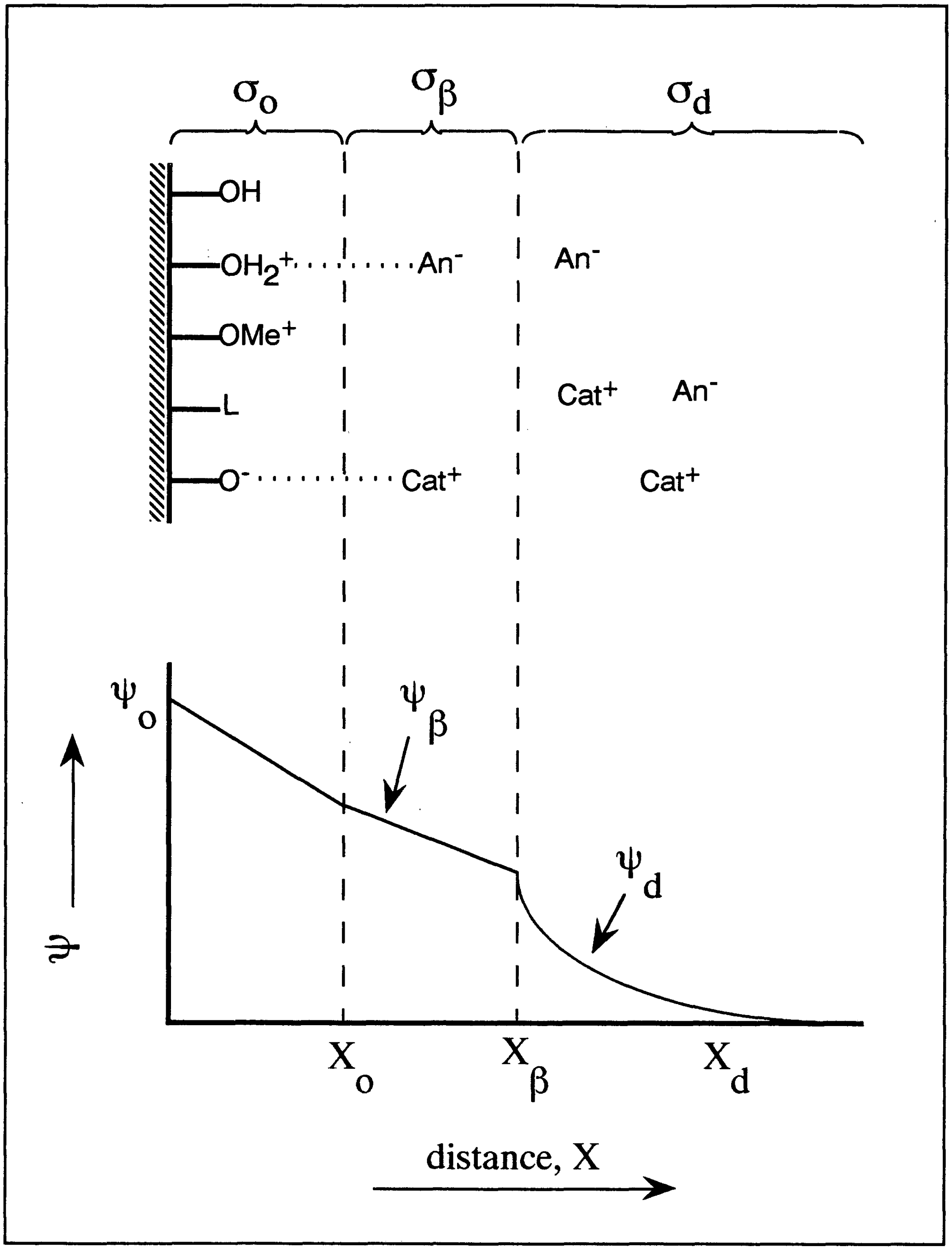

Figure 2.4 Triple-Layer Model (TLM) configuration of the oxide/water interface.

water column. These studies have traditionally used filter pore sizes of 0.2 - 1 μm to define dissolved and particulate species. In using this operational size definition, submicron colloidal matter (1,000 MW - 0.4 μm) is included in the dissolved phase. More recent studies in this area have utilized ultrafiltration techniques that allow particle size fractionation down to 1,000 nominal molecular weight. These studies indicate that 2 to 80% of the Th(IV) is associated with the colloid size fraction (1 nm - 2 μm; Niven and Moore, 1987; Baskaran *et al.*, 1992; Benner *et al.*, 1992; Moran and Buessler, 1993). This finding demonstrates that much of the thorium previously considered to be "dissolved" is, in fact, a constituent of the colloid pool.

Laboratory studies of thorium adsorption have utilized a variety of sorbent surfaces including metal oxides, natural particles, and humic materials. A summary of Th(IV) laboratory adsorption experiments in included in Table 2.1. These studies indicate that thorium adsorption by metal oxides is rapid and highly pH dependent, with fractional adsorption increasing with increasing pH. Both inorganic and organic ligands in solution can form complexes with aqueous Th(IV), and have variable effects on sorption depending on whether the complex is surface active (LaFlamme and Murray, 1987; Hunter *et al.*, 1988). Thorium adsorption by natural particles has been found to be rapid and reversible (Moore and Hunter, 1985; Moore and Millward, 1988; Niven and Moore, 1993), although in these studies desorption was not explicitly measured, or could be explained as particle disaggregation/coagulation rather than desorption. Thorium is strongly complexed by terrestrial humic and fulvic materials ([ThHum]/[Th] = 10^{10}), an interaction that occurs with carboxylate sites and that increases with polyelectrolyte ionization (Nash and Choppin, 1980; Cacheris and Choppin, 1987). Measured Th/COM associations indicate that Th(IV) is more weakly bound to marine colloidal material (Baskaran, *et. al.*, 1992; Moran and Buessler, 1993).

The adsorption of organic matter by mineral oxide surfaces is a process that can alter mineral oxide surface characteristics, and therefore, adsorption of trace metals by the surface. Adsorption of lake water and surface sediment organic matter by hydrous iron oxides exhibits ligand-like adsorption behavior (Tipping, 1981; Davis, 1982) and occurs by complex formation between surface hydroxyls and acidic functional groups of the organic matter. The extent of organic material adsorption is dependent on the nature of the surface, pH, sorbent/sorbate ratio and inorganic electrolyte composition. In some cases,

Table 2.1: Summary of Th(IV) laboratory sorption experiments

Authors	System	Conclusions	Implications
LaFlamme and Murray (1987)	goethite $NaNO_3$ electrolyte	Th surface complexes compete against non-sorbing Th hydroxy and Th carbonato (at high C_T) complexes	Non-sorbing Th complexes may significantly affect Th scavenging. Emphasizes role of solution chemistry.
Niven & Moore (1987)	alumina treated seawater	Likely existence of colloidal intermediate in sorption process. Up to 75% of "dissolved" Th is colloidal.	Rate limiting step in "sorption" may be colloid aggregation.
Hunter *et al.* (1988)	goethite, (δ-MnO_2) NaCl electrolyte	Th sorption unaffected by Mg^{+2}, Ca^{+2}, but Th/SO_4^{-2}, Th/EDTA solution phase complexes compete against surface complexes	Emphasizes role of solution chemistry.
Honeyman and Santschi (1989, 1991)	goethite, hematite simple electrolytes	Coagulation is rate controlling step	Scavenging rates can be predicted by coupling particle dynamics and surface chemistry
Niven & Moore (1993)	alumina treated seawater seawater pH	Rapid formation of polymeric Th hydroxide species. Sorption consistent with surface complexation. Reversibility presumed, not measured.	Implicates scavenging rate control by inorganic colloids
Nyffeler et al. (1984); Li et al. (1984); Jannasch et al. (1988)	natural particles complex matrices	Sorption kinetics a function of particle concentration, contact time. Desorption constants not explicitly measured	Sorption kinetics must be considered for systems with particle residence times of a few days or less.
Moore and Hunter (1985)	marine sediments seawater	Sorption is reversible: initially fast then slower rate steps. Th association with small <1 µm particles is negligible for natural systems	Support for reversible scavenging models
Moore and Millward (1988)	marine particles seawater	Th sorption is reversible. Reversibility decreases with particle aging.	Supports reversible scavenging models but data may suggest disaggregation/coagulation rather than desorption.
Moran and Moore (1989)	surface seawater	Fraction of "dissolved" Th in colloids is a function of DOC. Up to 50% of "dissolved" Th is colloidal.	Further support for the possible dominance of colloidal Th in the DOC pool.
Moran and Moore (1992)	dead diatoms seawater	Complex sorption kinetics; reversibility deduced from adsorption/equilibrium data but not explicitly measured by experiment.	Scavenging rate and extent controlled by colloidal intermediate. Diatoms strongly sorb Th. Support for the colloidal pumping model.
Nash and Choppin (1980)	humics and fulvics I = 0.1 M	Th binding with carboxylate sites; complexation increases with increasing polyelectrolyte ionization	Suggests Th fractionation within the COC pool according to binding site availability and type
Cacheris and Choppin (1987)	lake humics I = 0.1 M	Surface and interior binding have different complexation/decomplexation rates; [ThHum]/[Th] = 10^{10}	Reversibility of Th/humate bonds depends on nature of organic and equilibrium time.

almost complete surface site occupancy by adsorbed organic material occurs (Davis, 1982). Organic matter is a significant component in most natural aqueous systems; therefore, these studies indicate that it may play an important role in determining the surface chemistry, and therefore adsorptive capabilities, of particulate matter in these systems.

This issue has been addressed experimentally. For example, COM concentration was found to be responsible for nearly all the observed natural variation in adsorption of reduced plutonium by suspended sediment particles in natural waters (Nelson *et al.,* 1985), and increased DOM (dissolved organic matter, i.e., < 1000 nominal molecular weight) and COM concentrations in seawater caused decreased adsorption of thorium on alumina particles (Niven and Moore, 1987). In both of these cases there was a negative correlation between organic matter concentration in the system and solute adsorption; in otherwords, solution phase species were favored over surface complex formation.

In contrast to the constant pH conditions studied by the researchers above, Davis (1984) studied the sorption of Cu(II) and Cd(II) in systems containing colloidal alumina and dissolved natural organic matter as a function of pH. His results indicate that the effect of organic matter on metal ion adsorption by colloidal alumina particles is dependent, in part, on the metal ion examined. For example, Cu(II) adsorption and solution speciation was so dominated by organic matter in the system, that the observed sorption edge was transformed from metal-like to ligand-like behavior with increasing organic matter. In contrast, Cd(II) adsorption in the same system was not significantly affected by organic matter. These results demonstrate that a thorough understanding of the organic matter sorption characteristics as well as metal-organic complexation in solution is required to model interactions between particles and solutes in natural systems.

2.3 Experimental system reactions and stoichiometries

In experimental systems consisting of simple electrolytes (as $NaClO_4$), solution phase hydrolysis reactions control Th(IV) speciation. In the absence of competing ligands, thorium hydrolysis can be represented by the distribution diagram in Figure 2.5. At pH values below 3, the free Th^{+4} ion is the dominant species in solution. From pH 3 to 4.5, the 1:1 and 1:2 hydroxy complexes predominate. Above pH 4.5, $Th(OH)_4$ is the major dissolved species. The corresponding stoichiometric equations for the formation of the

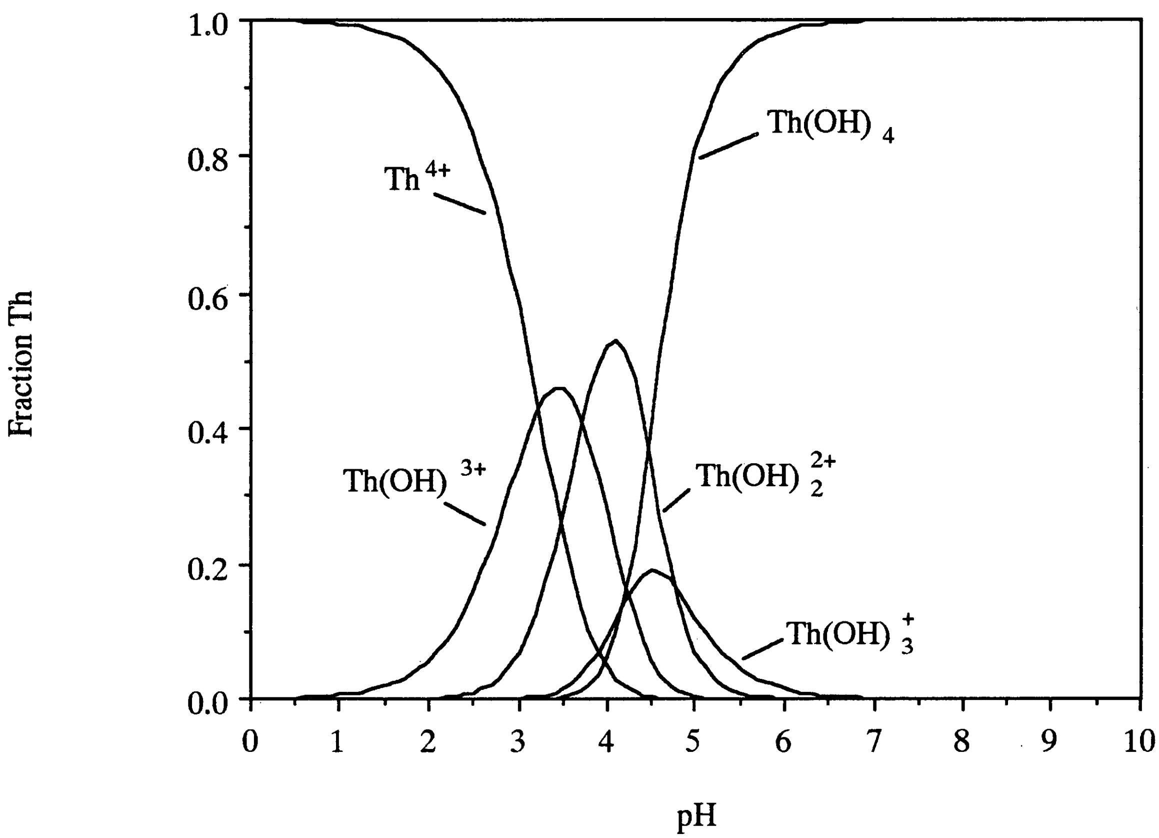

Figure 2.5 Calculated distribution of Th(IV) solution species as a function of pH.

hydroxylated species are given in Table 2.2.

Hematite surface reactions consist of surface protolysis, electrolyte reactions and complexation reactions. The surface complexes and reaction stoichiometries considered for TLM calculations are given in Table 2.3. Parameters required for TLM computations and values for hematite are summarized in Table 2.4.

Table 2.2 Solution phase reaction mass action expressions and stability constants for Th(IV) (LaFlamme and Murray, 1987).

Species	Reaction Stoichiometry	Expression	log K
$ThOH^{3+}$	$Th^{4+} + H_2O = ThOH^{3+} + H^+$	$[ThOH^{3+}][H^+] / [Th^{4+}]$	-3.22
$Th(OH)_2^{2+}$	$ThOH^{3+} + H_2O = Th(OH)_2^{2+} + H^+$	$[Th(OH)_2^{2+}][H^+] / [ThOH^{3+}]$	-3.72
$Th(OH)_3^{+}$	$Th(OH)_2^{2+} + H_2O = Th(OH)_3^{+} + H^+$	$[Th(OH)_3^{+}][H^+] / [Th(OH)_2^{2+}]$	-4.76
$Th(OH)_4^{0}$	$Th(OH)_3^{+} + H_2O = Th(OH)_4^{0} + H^+$	$[Th(OH)_4^{0}][H^+] / [Th(OH)_3^{+}]$	-4.17

Table 2.3 Surface complexes and reaction stoichiometries considered for TLM calculations. COM surface complex reaction stoichiometries are given in Section 4.3.

Reaction type	Reaction Stoichiometry
Surface protolysis	$SOH + H^+ = SOH_2^+$
	$SOH = SO^- + H^+$
Surface electrolyte reactions	$SOH + Na^+ = SO{-}Na^+ + H^+$
	$SOH + H^+ + ClO_4^- = SOH_2^+{-}ClO_4^-$
Surface complexation reactions	$SOH + Th^{4+} = SOTh^{3+} + H^+$
	$SOH + Th^{4+} + H_2O = SOThOH^{2+} + 2H^+$
	$SOH + Th^{4+} + 2H_2O = SOTh(OH)_2^+ + 3H^+$
	$SOH + Th^{4+} + 3H_2O = SOTh(OH)_3^0 + 4H^+$
	$SOH + Th^{4+} + 4H_2O = SOTh(OH)_4^{-1} + 5H^+$

Table 2.4 Triple-Layer Model parameters used for hematite.

Parameter	Value	Source
Specific Surface area (m^2/L)	9.54	This work
Site Density(nm^{-2})	2.3	Dzombak and Morel, 1990
Site Concentration (moles/L)	2.73×10^{-6}	This work
Inner Capacitance (F/m^3)	1.2	(a)
Outer Capacitance (F/m^3)	0.2	(a)
log $K_{a,1}$	6.7	Breeuwsma, 1972
log $K_{a,2}$	-10.3	Breeuwsma, 1972
log K_{cat}	-9.5	Breeuwsma, 1972
log K_{anion}	7.5	Breeuwsma, 1972

(a) These values fall within the range of commonly-used capacitances (Kohler *et al.*, 1992).

Chapter 3

MATERIALS AND METHODS

The materials and methods used in this research fall into three groups: 1) materials preparation, 2) experimental methods and, 3) quantification technique. This chapter describes these techniques and provides information on where to obtain more detail if desired. Sections 3.1 - 3.5 provide information on the procedures used to prepare the materials used in the experiment, Sections 3.6 - 3.10 outline the experimental procedures employed and Section 3.11 describes the method used for radionuclide quantification.

3.1 Thorium preparation (separation from uranium)

The thorium used in this research was supplied by M. Quigley (Texas A & M University) and prepared using the procedure described in Quigley *et al.* (manuscript in preparation). The method of separating ^{234}Th from its parent compound, ^{238}U, used uranyl acetate as the ^{234}Th source. Uranyl acetate was pretreated (hot acid digestions in 9 N HCl) prior to ion exchange chromatography. The resulting uranyl acetate was dissolved in 9 M HCl and passed through a pre-equilibrated (9 M HCl) BioRad AG 1-X8 chloride form, 100-200 mesh anion exchange resin column. Thorium was eluted with 9 M HCl, evaporated to dryness, then redissolved in 9 M HCl and passed through a second column of the same resin type. Thorium was eluted from this column with 9 M HCl, evaporated to dryness, then subjected to two hot acid digestions (8 M HNO_3) to oxidize any organic material that may have been present in the sample. The resulting thorium was dissolved in 8 M HNO_3 and applied to a pre-equilibrated (8 M HNO_3) anion exchange resin of the same type previously described. The column was washed with 8M HNO_3 and ^{234}Th eluted with 1 M HCl. This sample was evaporated to dryness, then subjected to three hot acid digestions (concentrated HNO_3) before dissolving the final evaporite in 2 mL concentrated HNO_3 and diluting with 8 mL distilled H_2O.

3.2 Hematite synthesis

Hematite (α-Fe_2O_3) was synthesized using the method described by Matijevic and Scheiner (1978) with slight modification. Several batches of hematite were made, each producing spherical particles of uniform size. The synthetic method entails incubating a solution of 0.018 M $FeCl_3$ in 4 mM HCl for 24 hrs. at 100 °C . Following incubation, the solution is cooled rapidly to room temperature and the sol formed repeatedly washed in 1 mM $HClO_4$ to remove amorphous α - Fe_2O_3. The hematite particles were stored in 1 mM $HClO_4$.

3.3 Marine Colloidal Organic Matter collection

Marine colloidal organic matter was provided by L. Guo (Texas A & M University). Surface (2 meter) seawater samples were collected from three stations along a transect at ~95.00° W during June, 1992 from the Gulf of Mexico, and fractionated by size following the method described by Guo *et al.*, 1993. Following collection, water samples were filtered (Whatman, GF/F) into precombusted glass bottles with Teflon lined caps, acidified (H_3PO_4) and frozen during storage. This material was then fractionated by size using a cross-flow ultrafiltration technique in which the seawater sample was first pumped through an acid rinsed 0.4 µm Nucleopore cartridge, then subjected to ultrafiltration using ultrafilter membranes with a nominal molecular weight cut-off of 1,000 Daltons. The colloidal organic matter concentrated by this filtration system is operationally defined as the fraction between 1,000 Daltons and 0.4 µm pore size. The concentrated colloidal fraction was then lyophilized producing a solid material that could be weighed out for experiments.

3.4 Marine Colloidal Organic Matter radiolabeling

Marine colloidal organic matter (COM) was radiolabeled following the method described by Wolfinbarger and Crosby (1983) for radiolabeling detritus. Slight modifications were made to the method due to the non-pelleting nature of aqueous COM suspensions when subject to centrifugation. The radiolabeling method utilizes the classical methylation reaction to methylate hydroxyl groups present in detrital material. The ether linkage so formed is reported to be stable to acid hydrolysis. Briefly, 8.25 mg COM was added to 100 μL 0.1 M NaOH solution containing 2.2 x 10^{-8} mmoles [^{3}H] dimethylsulfate. The reagents were allowed to react for 40 minutes at room temperature before reaction termination by dilution with Nanopure water. The reaction mixture was subjected to dialysis in Spectra/Por 7 membranes with a 1000 MW cutoff. The semi-permeable membrane allows unreacted [^{3}H]dimethylsulfate (MW 126.13) to diffuse through the membrane into a surrounding medium of Nanopure water, while radiolabeled colloids (1000 MW to 0.4 μm) are retained within the dialysis membrane. The sample was subjected to multiple, sequential "washes" in this manner until the Nanopure water surrounding the membrane exhibited no additional decrease in ^{3}H activity. The solution containing the radiolabeled COM was quantitatively transferred to a glass vial with a Teflon lined lid and stored at 2.5 °C for future use. Specific activity of ^{3}H COM stock was 76 nCi/mg COM.

3.5 Di 2-ethyl hexyl orthophosphoric acid purification

Di 2-ethyl hexyl orthophosphoric acid (HDEHP) was purified from a mixture of the di-octyl and mono-octyl esters following the method described by Peppard *et al.*, (1957) with slight modification. The purification protocol utilizes diethyl ether and ethylene glycol as opposing phases for the liquid/liquid partitioning separation of the two esters. The mono-octyl ester partitions into the ethylene glycol phase and the di-octyl ester (MW 322.7) partitions into the ether phase. Appropriate quantities of ethylene glycol (EG), diethyl ether (DEE) and unpurified HDEHP (Sigma Chemical Company) were combined in a 1 liter separatory funnel to give a EG/DEE/HDEHP ratio of 56/7/37 (v/v). Following partitioning, the ethylene glycol phase was removed from the separatory funnel and the remaining diethyl ether washed with water to remove traces of ethylene glycol. The diethyl ether phase was subsequently evaporated from the HDEHP/ether mixture, and the resulting purified HDEHP stored at room temperature for subsequent use.

3.6 Potentiometric titrations

Titrations of marine colloidal organic carbon (COM) and hematite suspensions were conducted under a nitrogen atmosphere in carbon dioxide depleted Nanopure water using a custom-designed potentiometric titrator (Redden Rocket; George Redden Enterprises; Menlo Park, CA). Solutions containing the desired amount of COM (0.165 g/L) or hematite (1g/L) were titrated with CO_2-free, standardized NaOH or HCl in a double-walled, closed 50 mL Celstir titration flask. Temperature was kept constant at 25 °C by circulation of water through the outer chamber of the titration flask. Ionic strength was adjusted with $NaClO_4$. Minimum volumes of 0.001 mL titrant were dispensed into the COM suspension with computer-controlled Gilmont burets. Suspension pH was monitored with an Orion pH meter/Ross combination electrode.

3.7 Adsorption of Th(IV) by hematite

Adsorption experiments were conducted in 50 mL Teflon centrifuge tubes. The centrifuge tubes were washed in 3 N HCl and rinsed with Nanopure water prior to the experiments. Solutions containing 4 x 10^{-15} M ^{234}Th and 74 ppm hematite were adjusted to the desired pH with HCl or NaOH. Ionic strength was adjusted to 0.01 or 0.1 M with $NaClO_4$. Total solution volumes were 20 mL. Two mL aliquots of the solution were added to 10 mL scintillation cocktail and quantified by liquid scintillation counting for total ^{234}Th activity. Free ^{234}Th was separated from adsorbed ^{234}Th by centrifugation at 2750 g for 30 minutes. Two mL aliquots of the supernatant were added to 10 mL scintillation cocktail and quantified by liquid scintillation counting of ^{234}Th. Bound ^{234}Th was calculated as [total solution ^{234}Th activity] - [free ^{234}Th activity].

3.8 Adsorption of ^{3}H COM by hematite

Adsorption experiments were conducted using Teflon centrifuge tubes as described above. Solutions containing 74 ppm hematite were adjusted to the desired pH with HCl or NaOH. COM stock was added to yield a 1.48 mg/L solution concentration. Total solution volumes were 20 mL. Two mL aliquots of the solution were added to 10 mL scintillation cocktail and quantified by liquid scintillation counting for total ^{3}H COM activity. After one hour at room temperature, adsorbed COM was separated from free ^{3}H COM by centrifugation as described above. Two mL aliquots of the supernatant were added to 10 mL scintillation cocktail and quantified by liquid scintillation counting of ^{3}H COM. Bound ^{3}H COM was calculated as [total solution ^{3}H COM activity] - [free ^{3}H COM activity].

3.9 Complexation of Th(IV) by COM

The Th(IV) solution for complexation experiments was prepared in a Teflon beaker. The beaker was washed in 3 N HCl and rinsed with Nanopure water prior to the experiments. A solution containing 4 x 10^{-15} M ^{234}Th was adjusted to the desired pH with HCl or NaOH. Ionic strength was adjusted with $NaClO_4$. At each pH, five mL aliquots of the Th(IV) solution were added to two polyethylene scintillation vials with plastic caps. Two mL aliquots of the solution were added to 10 mL scintillation cocktail and quantified by liquid scintillation counting for total ^{234}Th activity. COM was added to one vial of each pair to give a COM solution concentration of 1.48 mg/L. Solutions were allowed to sit at room temperature for one hour. ^{234}Th- COM complexes were separated from free ^{234}Th following the method described by Nash and Choppin, 1980. This technique separates ^{234}Th-COM complexes from free ^{234}Th by liquid/liquid partitioning of the aqueous solution with an organic phase (HDEHP in toluene). The organic phase was HDEHP in toluene at concentrations suitable to obtain distribution coefficients (organic ^{234}Th activity/aqueous ^{234}Th activity) of 1 (5 - 500 nM HDEHP). Five mL organic phase were added to each pair of aqueous solutions and shaken for at least 60 hours to ensure equilibrium. The vials were centrifuged at 500 rpm for 5 minutes to expedite phase separation. Two mL aliquots were taken from the aqueous phase (^{234}Th- COM complexes) and quantified by liquid scintillation counting of ^{234}Th. Free ^{234}Th was calculated as [total solution ^{234}Th activity] - [bound ^{234}Th activity].

3.10 Adsorption of Th(IV) by hematite in the presence of ^{3}H COM

Adsorption experiments were conducted in Teflon centrifuge tubes as described above. Solutions containing 4 x 10^{-15} M ^{234}Th were adjusted to the desired pH with HCl or NaOH. Ionic strength was adjusted to 0.01 or 0.1 M with $NaClO_4$. COM stock was added to yield a 1.48 mg/L solution concentration and the solutions allowed to sit at room temperature for one hour. Hematite stock was then added to the solutions to yield a 74 ppm solution concentration. Total solution volumes were 20 mL. Total ^{234}Th activity was taken as described above, and solutions were again allowed to sit at room temperature for one hour. Free ^{234}Th was separated from adsorbed ^{234}Th and quantified as previously described. Adsorbed ^{234}Th was calculated as [total solution ^{234}Th activity] - [free ^{234}Th activity]. Mass balances were conducted to ensure that total ^{234}Th activity was the sum of the bound and unbound activities.

3.11 Radionuclide quantification by liquid scintillation counting

A two mL aliquot of the sample to be quantified was added to ten mL liquid scintillation cocktail (Ultima Gold XL). Measurements were performed on a Packard Liquid Scintillation counter, Model 1600TR. Quench curves for the conversion of cpm to dpm values were constructed using hematite as the quenching agent. Background samples contained two mL Nanopure water and 10 mL scintillation cocktail.

Chapter 4

EXPERIMENTAL AND MODELING RESULTS

This chapter contains the results of experiments investigating the adsorption of Th(IV) by hematite in the presence of marine colloidal organic matter. Our experimental approach consisted of four basic objectives: 1) define the physicochemical properties of the sorbent/complexants (hematite and COM), 2) evaluate adsorption in binary combinations of the ternary system components, 3) evaluate Th(IV) adsorption in the ternary system, and 4) understand adsorption of Th(IV) in ternary systems in terms of the individual component processes. The experimental results for these tasks are presented in this chapter. Modeling results (TLM) for individual component processes and the ternary system follow their respective experimental results.

4.1 Surface characterization

Several sorbent properties influence solute adsorption from solution. These properties must be characterized to properly interpret adsorption data. Sorbent properties include particle size and morphology, surface area, chemical composition and site density of functional groups. The following sections describe experimental results for the characterization of hematite and COM sorbent properties.

4.1.1 Hematite

Hematite particle size and morphology was determined by scanning electron microscopy (courtesy B. Klug and B. McGrew, Department of Metallurgy, Colorado School of Mines). Electron micrographs (Figure 4.1 and 4.2) revealed homogeneous, spherical hematite particles with an average diameter of 120 nm. This size and morphology is consistent with the synthetic method employed. Specific surface area of the hematite

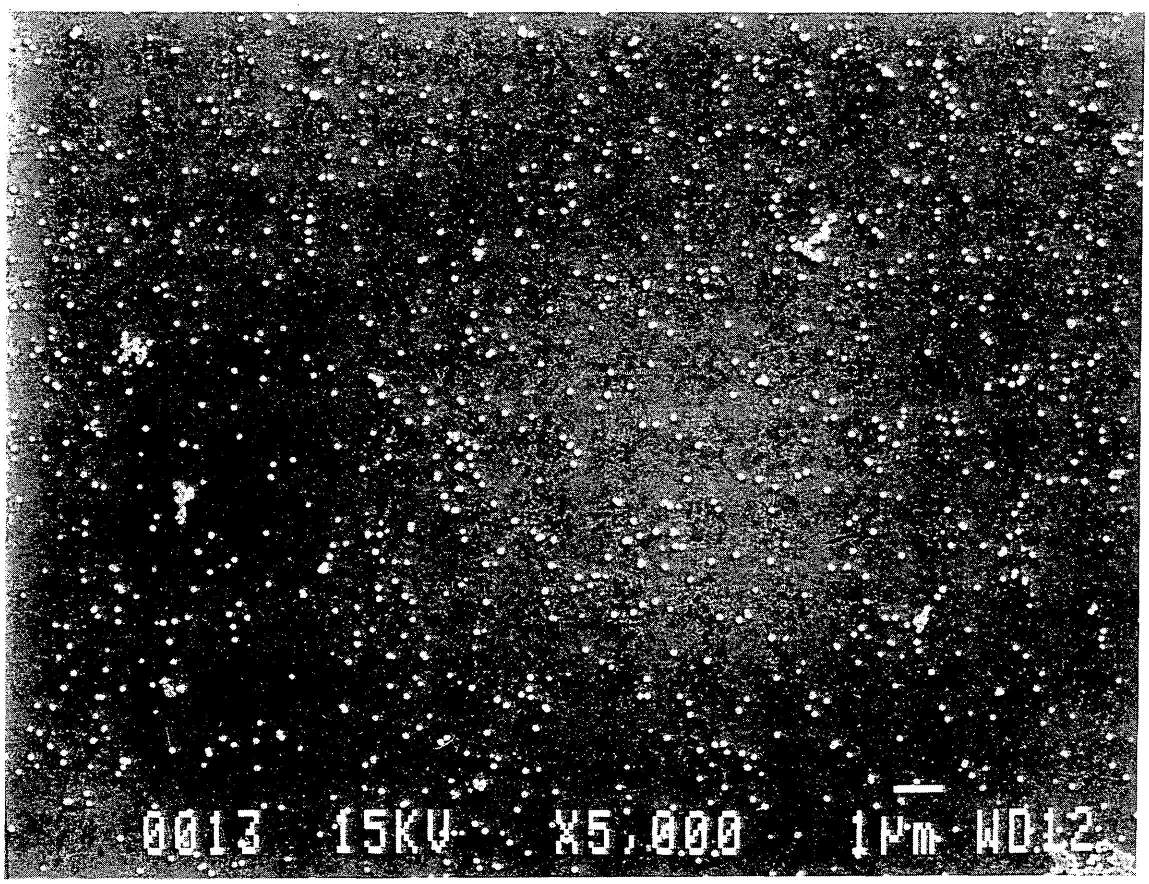

Figure 4.1 Scanning electron micrograph of hematite particles; x5000

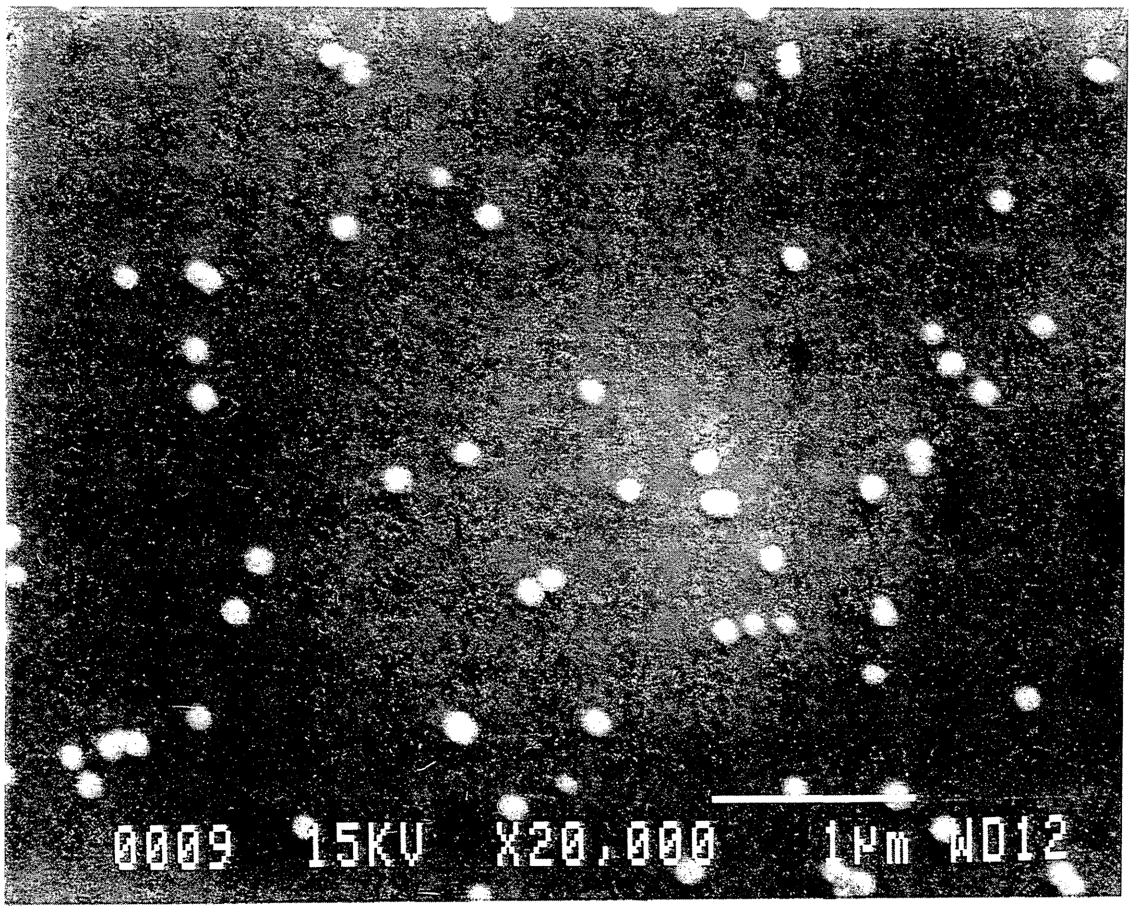

Figure 4.2 Scanning electron micrograph of hematite particles; x20,000

particles was calculated to be 9.54 $m^2\ g^{-1}$, which is similar to those reported in the literature for iron oxides (Penners, 1985; Liang, 1988).

Site density (sites nm^{-2}) of surface functional groups was determined by potentiometric titration (Figure 4.3). This technique allows the maximum proton uptake or release at extreme pH values to be obtained from acid-base titration data (Dzombak and Morel, 1990). Titration curves were transformed to proton saturation isotherms (log Γ versus log H^+) by mathematically correcting the titration data for water effects and normalizing for the amount of hematite present (Figure 4.4). The calculated site density (5.75 sites nm^{-2}) falls within the range reported in the literature for iron oxides (Hayes *et al.*, 1988). A site density of 2.31 sites nm^{-2}, however, was used in modeling efforts for two reasons: 1) to comply with efforts to develop a self-consistent data set for trace element adsorption in complex mixtures of sorbents and 2) because there is evidence in the literature indicating that the ability of surface complexation models to fit adsorption data is relatively insensitive to variations in site density (Honeyman, 1991).

4.1.2 Marine Colloidal Organic Matter

Colloidal material characterization consisted of percent inorganic component, percent carbon (C) and site density (moles sites g^{-1} COM) determinations. Percent inorganic component was determined by muffle oven combustion (550 °C) of a COM sample. Results show that 83.5% (by weight) of the COM is an inorganic component which indicates a significant seasalt constituent in the COM. Both percent carbon and site density calculations were corrected for this constituent in the sample. The corrected concentration of carbon in the COM was determined to be ~0.12 mg C/mg COM (courtesy L. Guo, Department of Marine Sciences, Texas A & M University). COM site density (moles sites g^{-1} COM) was determined by potentiometric titration (Figure 4.5) and subsequent transformation to a proton saturation isotherm (Figure 4.6). This method gave a site density of ~1.44 x 10^{-3} moles sites g^{-1} COM. This estimate is similar to values reported in the literature for marine COM site density, i.e., 1 mole/ kg (Balistrieri *et al.*, 1981).

The inflections in the COM proton saturation isotherm curve are caused by heterogeneity of functional groups present in the COM sample. Although a number of

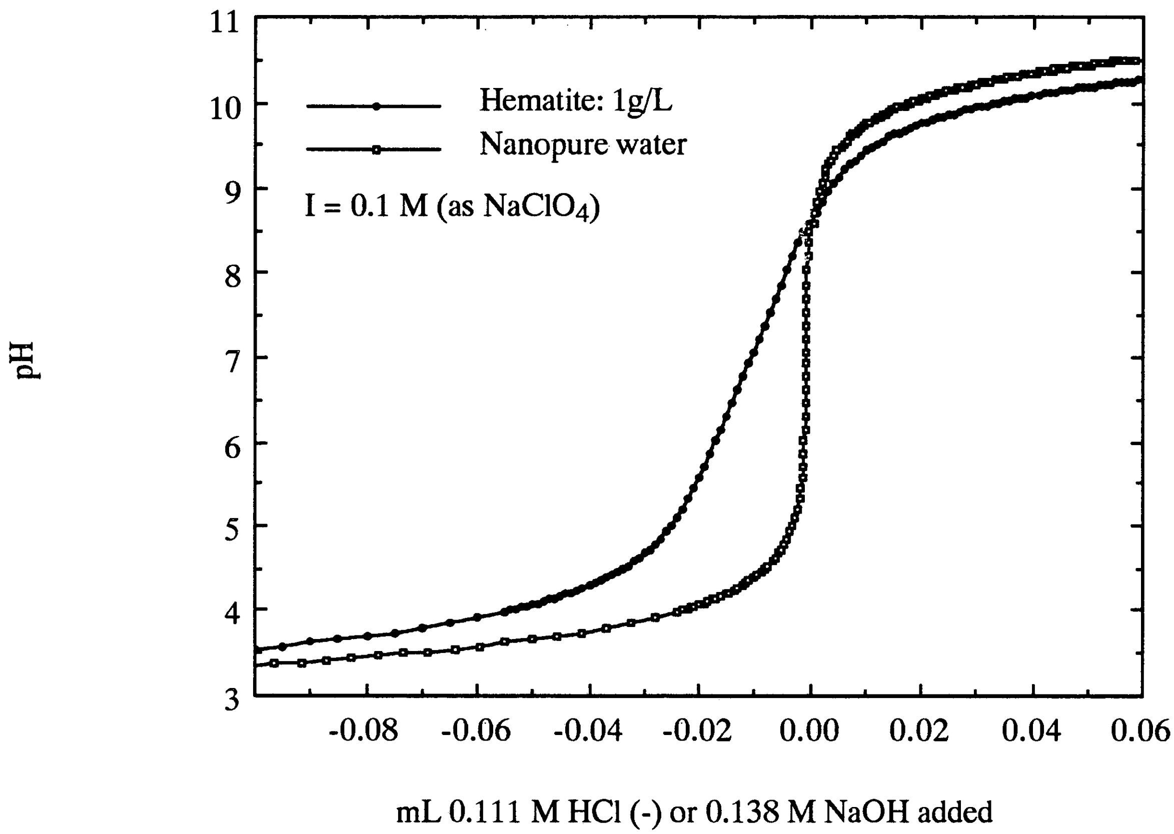

Figure 4.3 Titration data as a function of pH for hematite (1g/L) with a background electrolyte concentration of 0.1 M as $NaClO_4$.

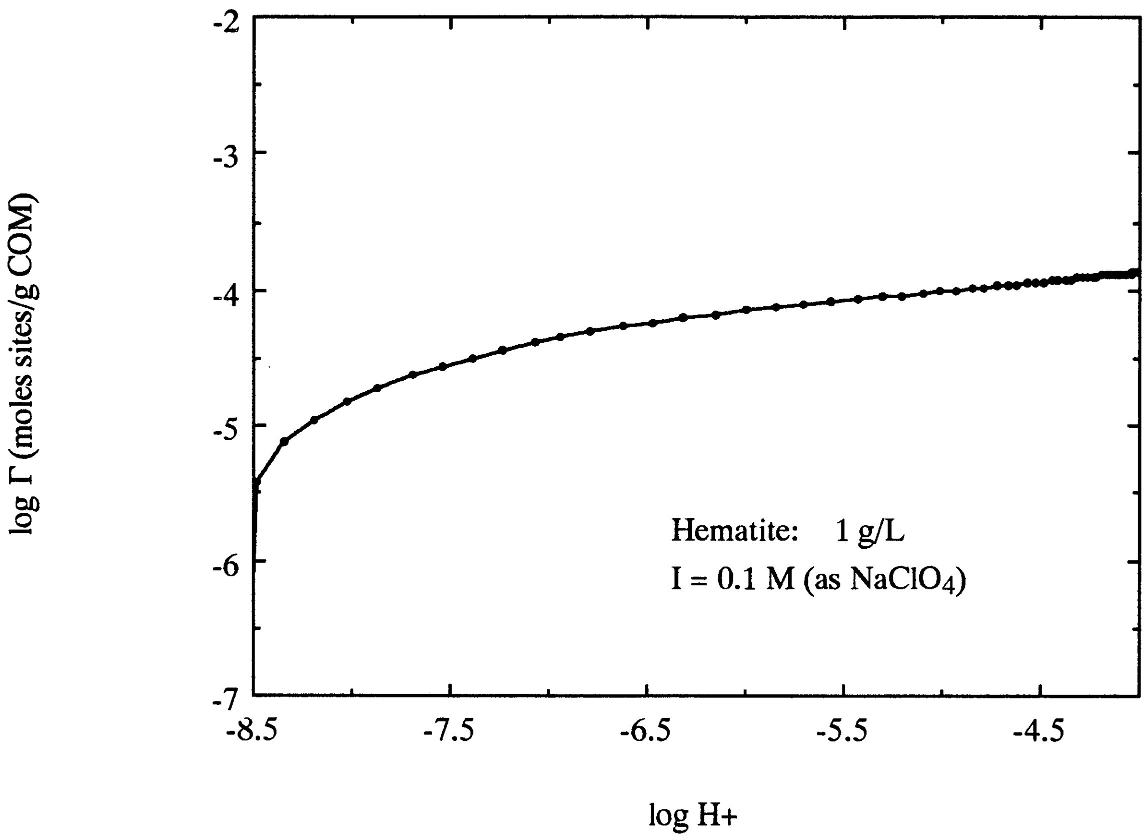

Figure 4.4 Computation of proton saturation isotherm (log Γ vs. log H^+) for hematite (1g/L) with a background electrolyte concentration of 0.1 M as $NaClO_4$.

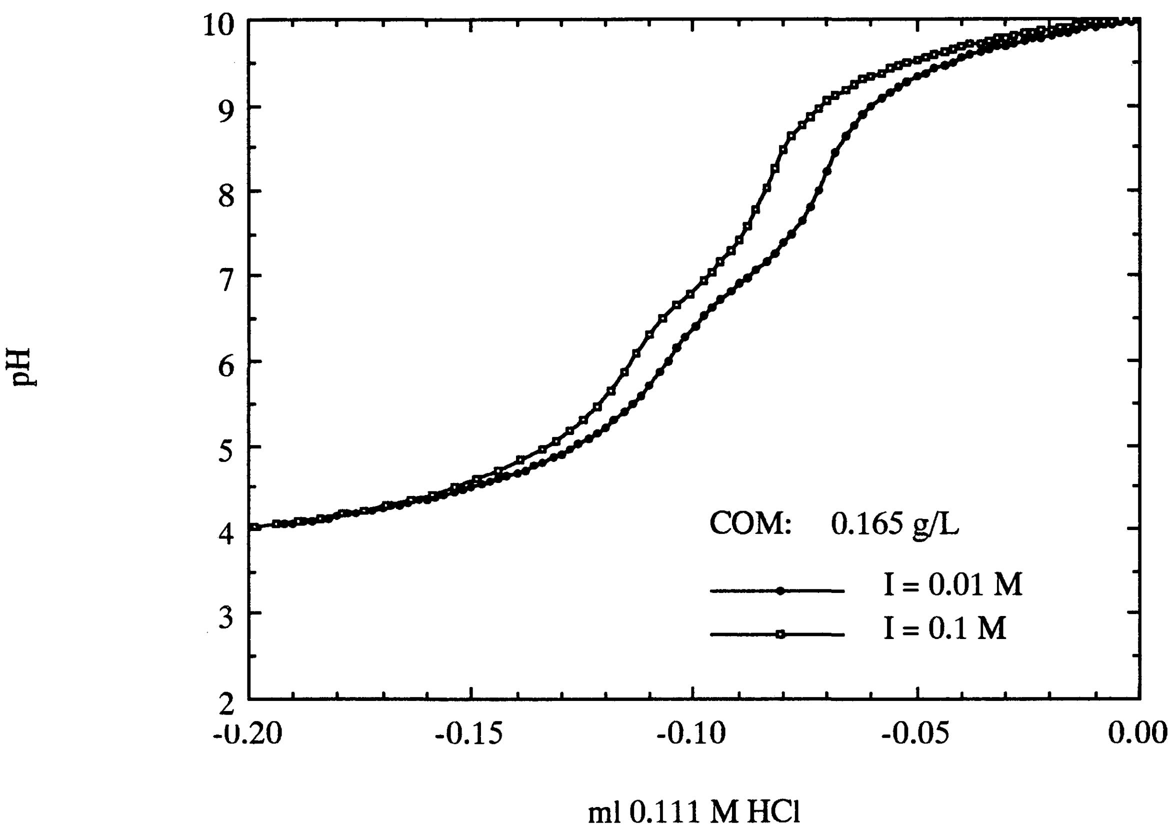

Figure 4.5 Titration data as a function of pH for colloidal organic matter (0.165 g/L) with a background electrolyte concentration of 0.01 and 0.1 M as $NaClO_4$.

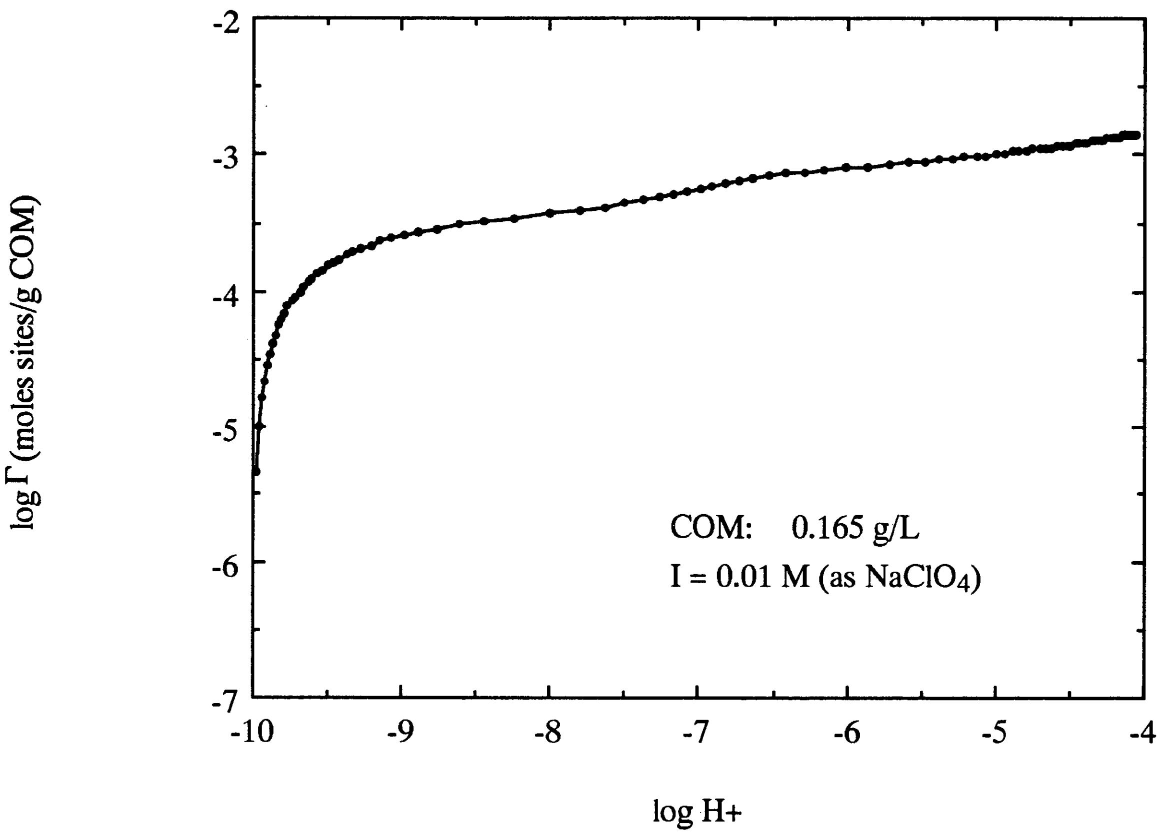

Figure 4.6 Computation of proton saturation isotherm (log Γ vs. log H^+) for colloidal organic matter (0.165 g/L) with a background electrolyte concentration of 0.01 M as $NaClO_4$.

methods are available in the literature for estimating the number and type of functional groups in natural organic matter (Gamble, 1970; Buffle *et al.*, 1990; Aleixo *et al.*, 1992; Manunza *et al.*, 1992), a more fundamental approach consists of simulating the proton saturation isotherm as the sum of several acid dissociation curves. Using this approach, the COM proton saturation isotherm was simulated with three theoretical monoprotic acid ligands. The dissociation constants (pK_a's) used for the ligands were 4.8, 7.1 and 9.6, and their concentrations 3.2, 3.3 and 3.5 moles/g COM, respectively. An illustration demonstrating the fit of the experimental data is provided in Figure 4.7.

4.2 Adsorption of Th(IV) by hematite

Th(IV) sorption by hematite was established experimentally and used as a "baseline" for evaluating the effects of COM on Th(IV) sorption. Experiments were designed to test the dependency of Th(IV) sorption on pH and ionic strength. Th(IV) fractional adsorption by hematite as a function of pH is shown in Figure 4.8. The increase in Th(IV) adsorption with increasing pH is characteristic of cation adsorption on metal oxides. The adsorption "edge" for 4 x 10^{-15} M Th(IV) and 2.73 x 10^{-6} M hematite lies between pH 2-5 and sorption behavior is consistent with other studies of thorium sorption on metal oxides (Quigley *et al.*, manuscript in preparation; LaFlamme and Murray, 1987; Hunter *et al.*, 1988). A thorough study of the effect of hematite and Th(IV) concentration on the position of the sorption edge and Th(IV) sorption and desorption kinetics is provided by Quigley *et al.* (manuscript in preparation).

The effect of variation in ionic strength on thorium fractional adsorption is illustrated in Figure 4.9. Although the data shows a slight shift of the sorption edge toward lower pH values with decreasing ionic strength, Th(IV) sorption appears to be relatively insensitive to changes in ionic strength, which suggests it occurs as an inner-sphere (o - plane) complex (Hayes and Leckie, 1987). However, in initial attempts to model Th(IV) sorption, all sorbing species were assigned to the β - plane (outer-sphere complexes). The model curve was fit to the data in a step-wise fashion starting with one sorbing species (Th^{+4}), and sequentially adding hydroxy species to the model. Log K^{int} or β^{int} values were adjusted until the slope of the model line fit the data before another species was added. Model results are illustrated in Figure 4.10. While the outer-sphere configuration fit

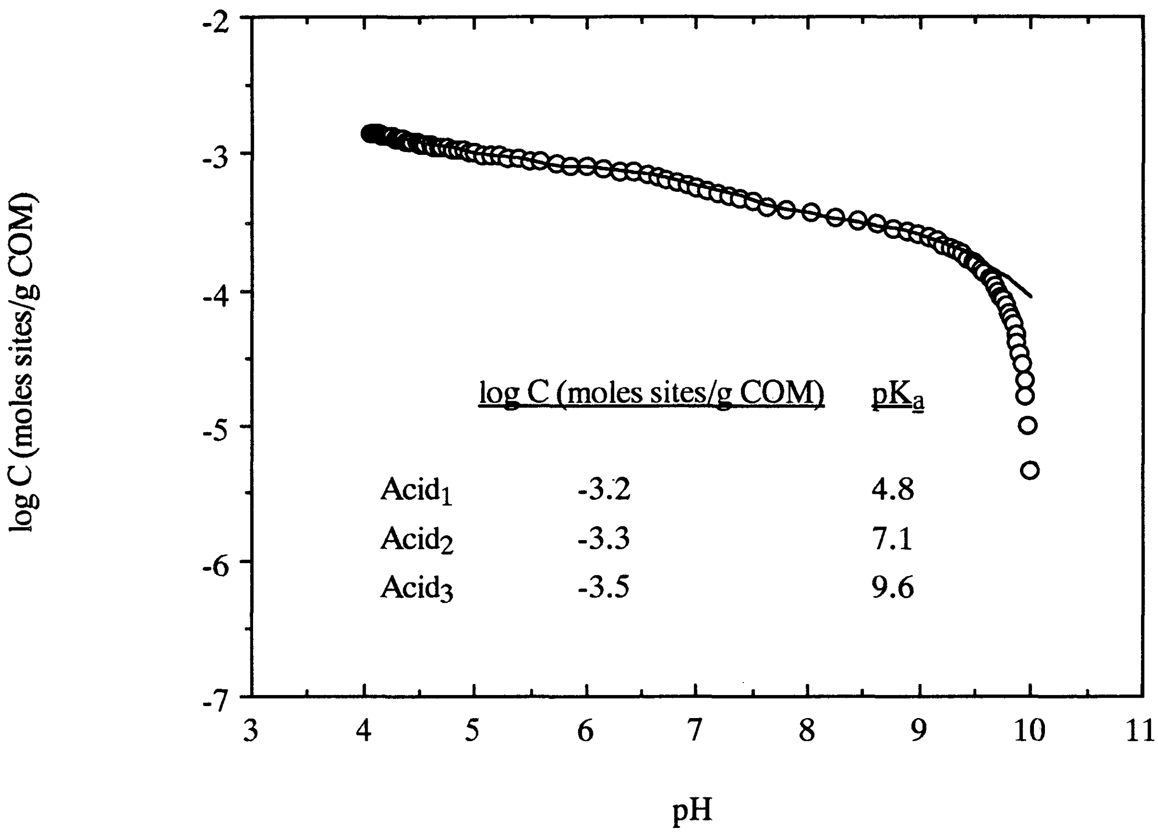

Figure 4.7 Simulation of COM proton saturation isotherm data with three monoprotic acid ligands. Open circles represent experimental data; solid line is simulation. Total sites: 1.44×10^{-3} moles/g COM.

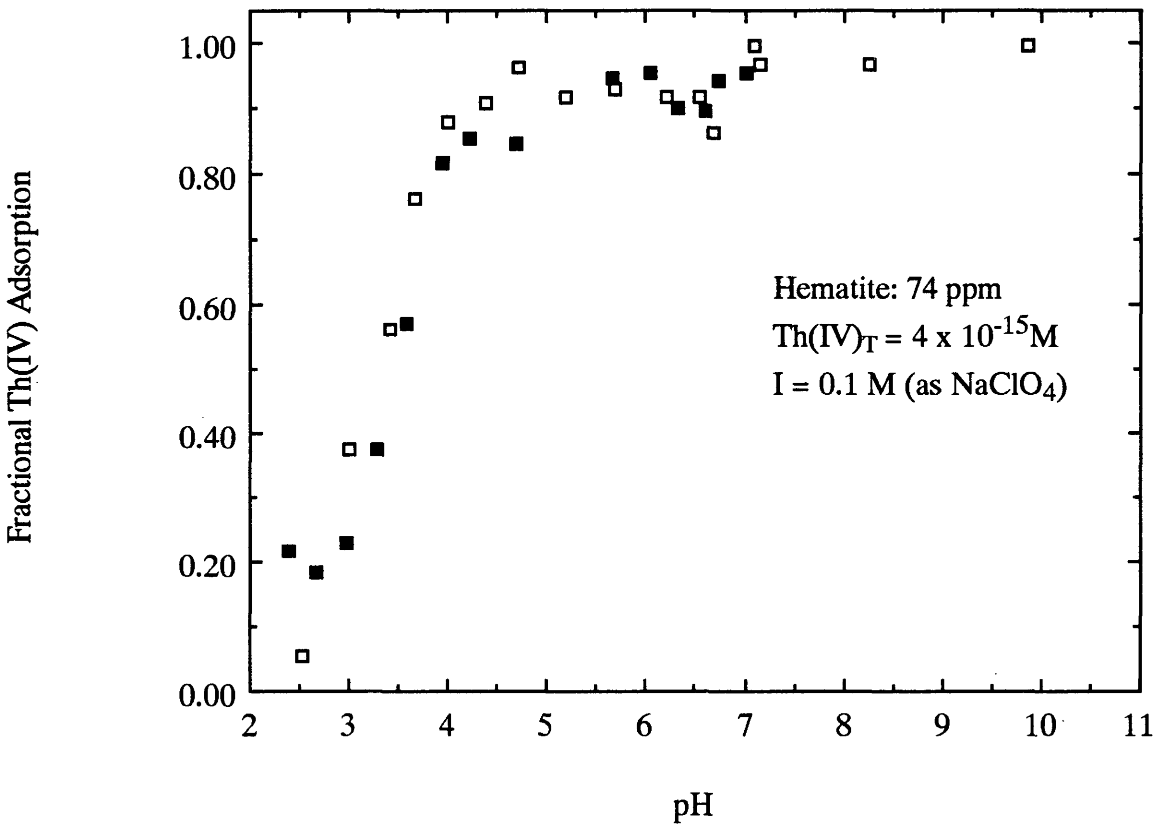

Figure 4.8 Equilibrium fractional Th(IV) sorption edge for 4×10^{-15} M total Th(IV) and 74 ppm hematite (2.73×10^{-6} M) with a background electrolyte concentration of 0.1 M as $NaClO_4$. Open and closed symbols indicate different experiments.

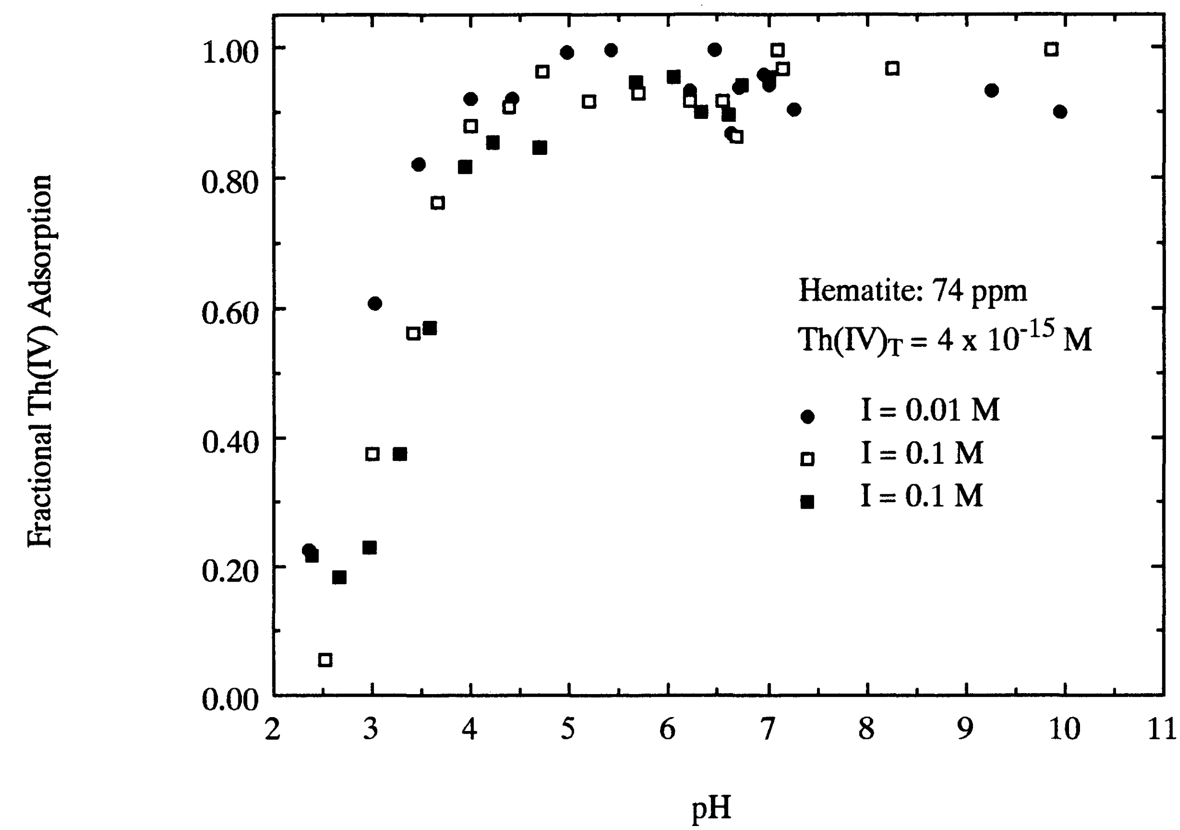

Figure 4.9 Effect of $NaClO_4$ concentration on equilibrium sorption of 4×10^{-15} M total Th(IV) by 74 ppm hematite (2.73×10^{-6} M) with a background electrolyte concentration of 0.01 and 0.1 M as $NaClO_4$.

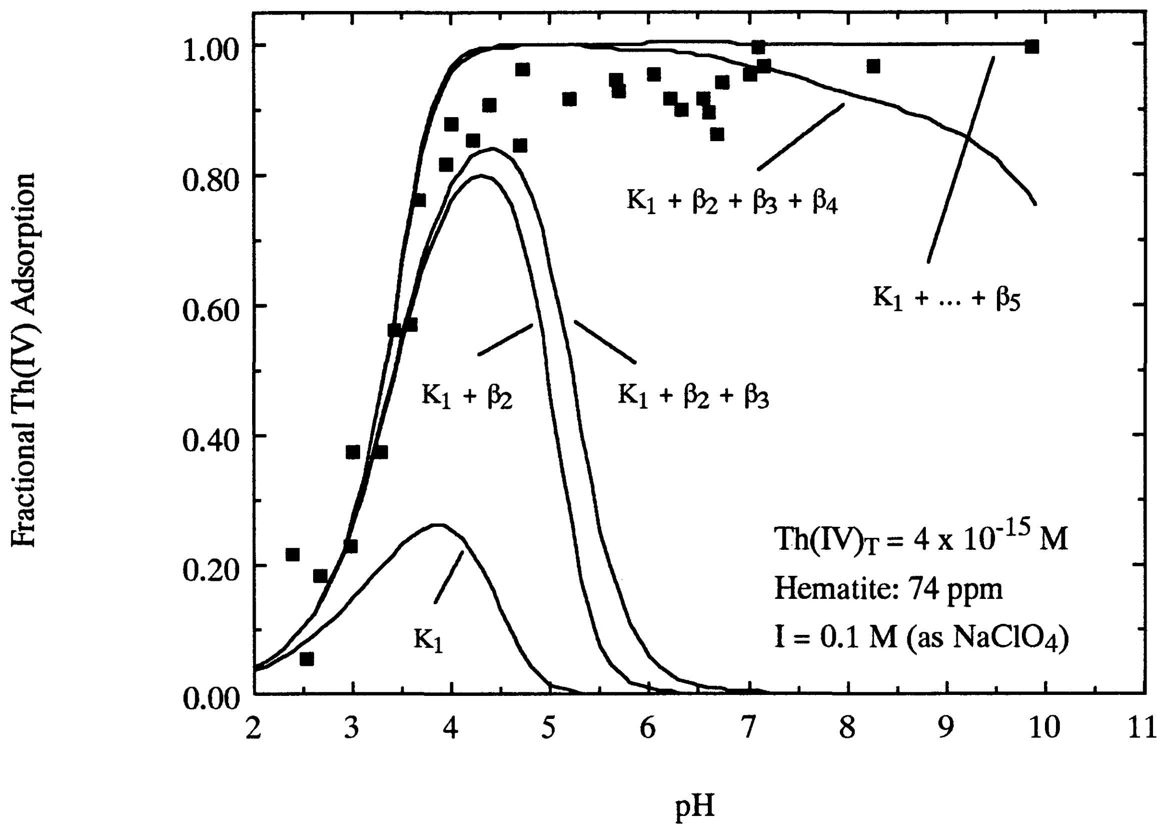

Figure 4.10 Fit of TLM data to experimental data using successive addition of outer-sphere thorium species for the equilibrium fractional adsorption of 4×10^{-15} M total Th(IV) by 74 ppm hematite (2.73×10^{-6} M).

of the data is adequate for 0.1 M ionic strength, the results failed to fit the experimental data at 0.01 M ionic strength as the model predicts a shift in the position of the adsorption edge toward higher pH values with lower ionic strength (Figure 4.11). The inability of the outer-sphere configuration to fit the experimental data at 0.01M ionic strength further supports the argument that Th(IV) sorbs on hematite as an inner-sphere complex.

The results of modeling thorium sorption as an inner-sphere complex are illustrated in Figure 4.12. Several surface complexation reactions are possible for thorium and hematite surfaces; however, the best fit of the data was obtained using one thorium inner-sphere complex:

$$SOH + Th^{+4} = SOTh^{+3} + H^{+} \qquad K^{*}_{int} = \frac{[SOTh][H^{+}]}{[SOH][Th^{+4}]} \exp\left\{\frac{3F\Psi_{o}}{RT}\right\}$$

$$\log K^{*}_{int} = 17.3$$

Adding any thorium hydroxy surface complexes to the model increased the sorption edge slope such that the predicted edge did not approximate the data.

The effect of ionic strength on the fit of TLM data to experimental data is illustrated in Figure 4.13. The model predicts less movement of the sorption edge toward lower pH values with decreasing ionic strength than was observed experimentally; however, both model data and experimental data suggest that Th(IV) binds as an inner-sphere complex.

4.3 Adsorption of ^{3}H COM by hematite

COM fractional adsorption experiments were designed to test the dependency of COM sorption on pH and ionic strength. The reagent used to radiolabel the COM ([^{3}H] dimethylsulfate) exhibited negligible sorption on hematite, therefore, all ^{3}H activity on the hematite was attributed to ^{3}H COM. Preliminary sorption rate experiments showed that COM sorption on hematite reaches equilibrium within one hour at room temperature. COM fractional adsorption as a function of pH is presented in Figure 4.14. Sorption is pH

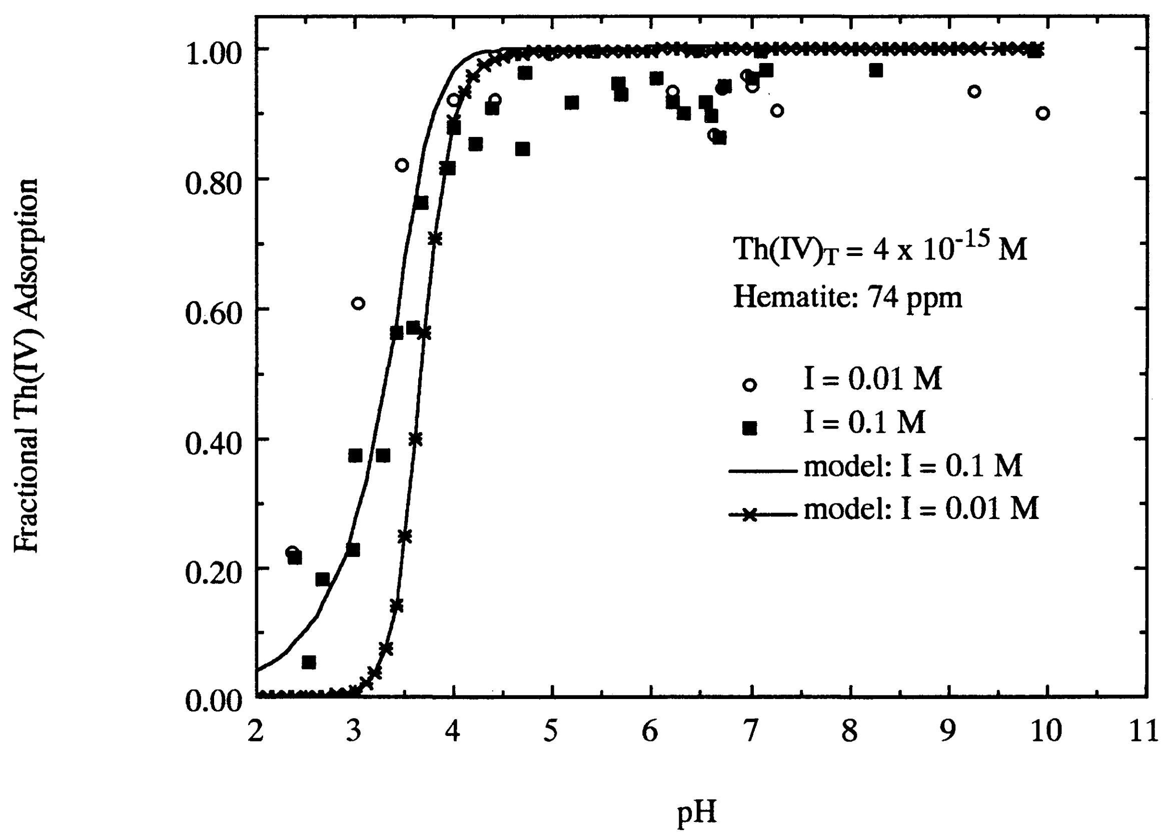

Figure 4.11 Effect of $NaClO_4$ concentration on fit of TLM data to experimental data using outer-sphere thorium species for the equilibrium fractional adsorption of 4×10^{-15} M total Th(IV) by 74 ppm hematite (2.73×10^{-6} M).

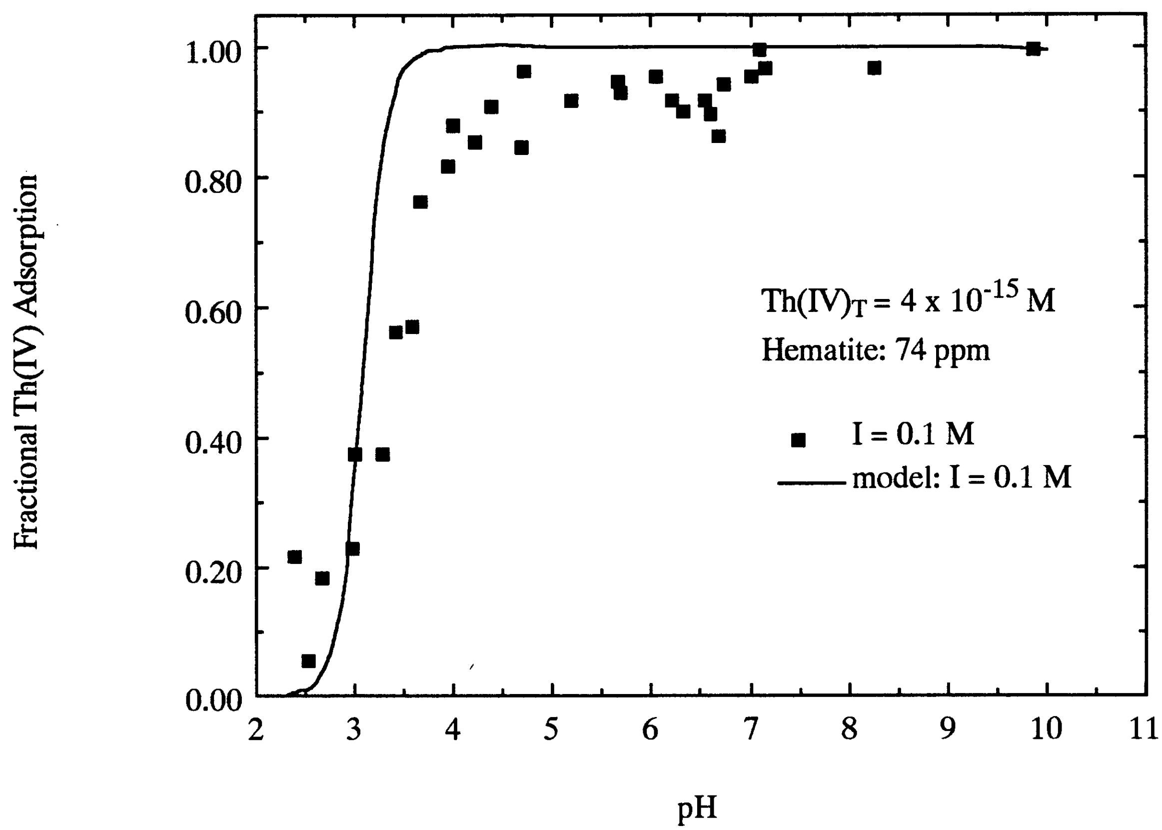

Figure 4.12 Fit of TLM data to experimental data using one inner-sphere thorium species for the equilibrium fractional adsorption of 4×10^{-15} M total Th(IV) by 74 ppm hematite (2.73×10^{-6} M) with a background electrolyte concentration of 0.1 M as $NaClO_4$.

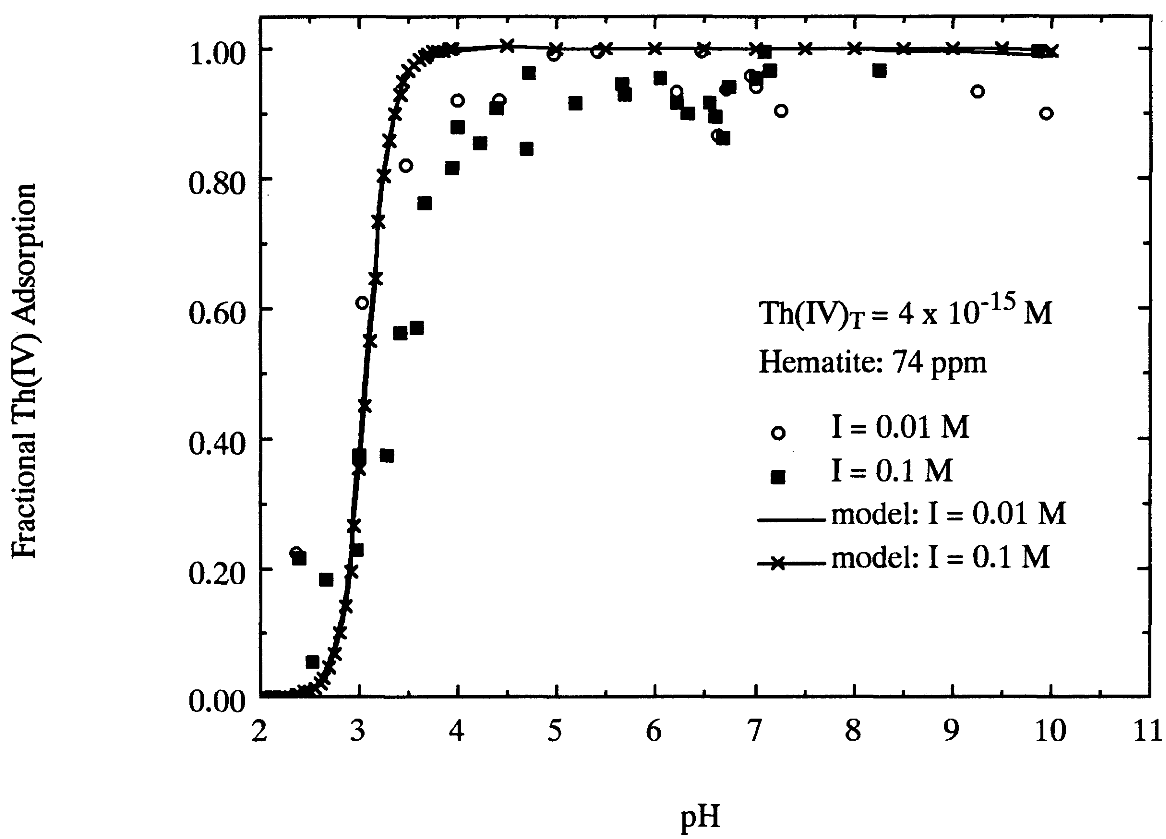

Figure 4.13 Effect of $NaClO_4$ concentration on fit of TLM data to experimental data using one inner sphere thorium species for the equilibrium fractional adsorption of 4×10^{-15} M total Th(IV) by 74 ppm hematite (2.73×10^{-6} M).

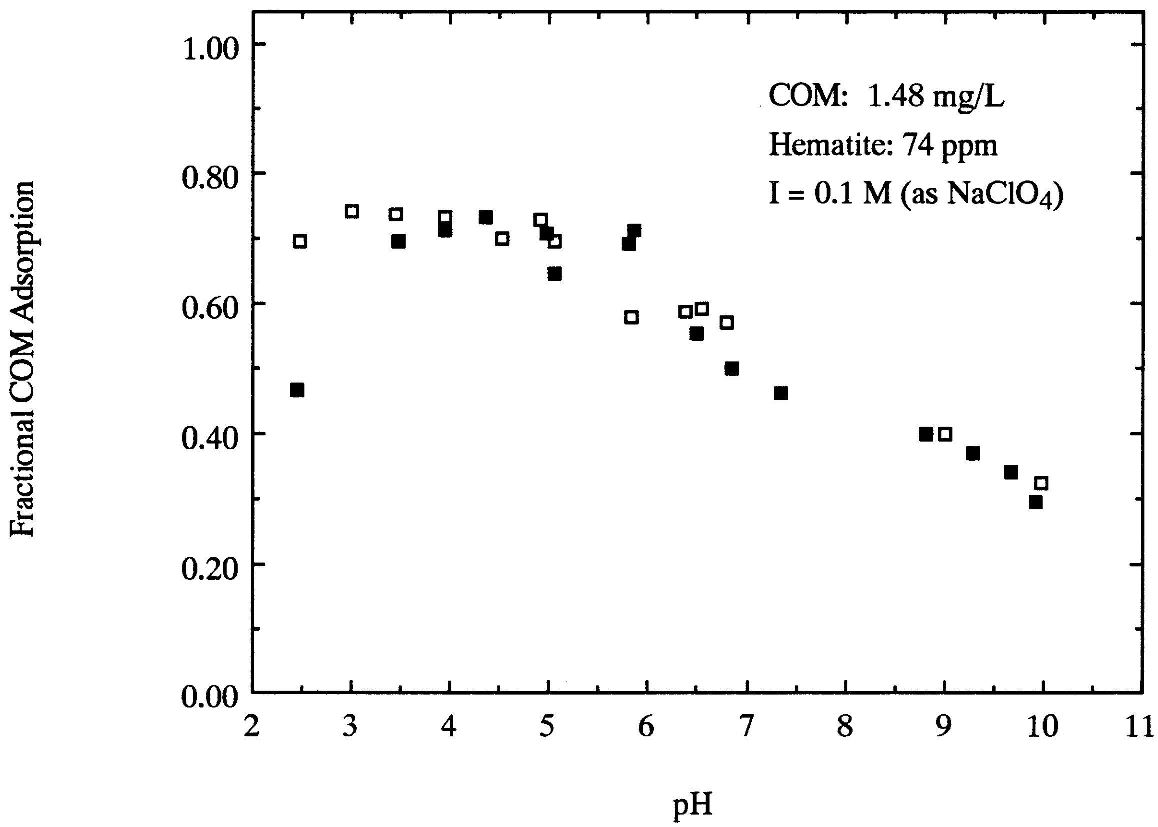

Figure 4.14 Equilibrium fractional COM sorption edge for 1.48 mg/L total COM and 74 ppm hematite (2.73 x 10^{-6} M) with a background electrolyte concentration of 0.1 M as $NaClO_4$.

dependent and exhibits "ligand-like" behavior, i.e., decreases with increasing pH. This observed behavior is compatible with studies of natural organic matter sorption on metal oxide surfaces (Davis, 1982; Tipping, 1981). The effects of variation in ionic strength on COM fractional adsorption is illustrated in Figure 4.15. Sorption appears to be relatively insensitive to changes in ionic strength, which suggests that like Th(IV) sorption by hematite, COM sorption by hematite occurs as an inner-sphere (o - plane) complex (Hayes et al., 1988). COM sorption on hematite was modeled using the Triple-Layer Model, treating the COM as a triprotic acid ligand with pK_a's of 4.8, 7.1 and 9.6, and a total site concentration of 1.44 x 10^{-3} moles/g COM. The following surface reactions were used to model the data:

$$SOH + H^+ + COM^{-3} = SOH_2COM^{-2} \qquad \log K^*_{int} = 19.2$$

$$SOH + 2H^+ + COM^{-3} = SOH_2COMH^{-1} \qquad \log \beta^*_{2,\,int} = 24.6$$

$$SOH + 3H^+ + COM^{-3} = SOH_2COMH_2 \qquad \log \beta^*_{3,\,int} = 29.1$$

The results of modeling COM sorption on hematite as an inner-sphere complex is illustrated in Figure 4.16. The model simulates the experimental data fairly well at low to mid pH values, but falls off at high pH values. Attempts to increase the model prediction on this end of the curve resulted in nonconformity to the experimental data in the other pH regions. This behavior is most likely due to representing the COM in the model as a triprotic acid ligand with one total site concentration. It would be more realistic to represent the COM as one ligand "backbone" composed of three functional groups of <u>different</u> concentrations, but this is not possible using the TLM at this time. The inner-sphere configuration provided the best fit to the data as attempts to model COM sorption on hematite using the outer-sphere configuration failed. At this time we have no explanation for the predicted shift of the sorption edge when modeling COM sorption on hematite using the inner-sphere configuration.

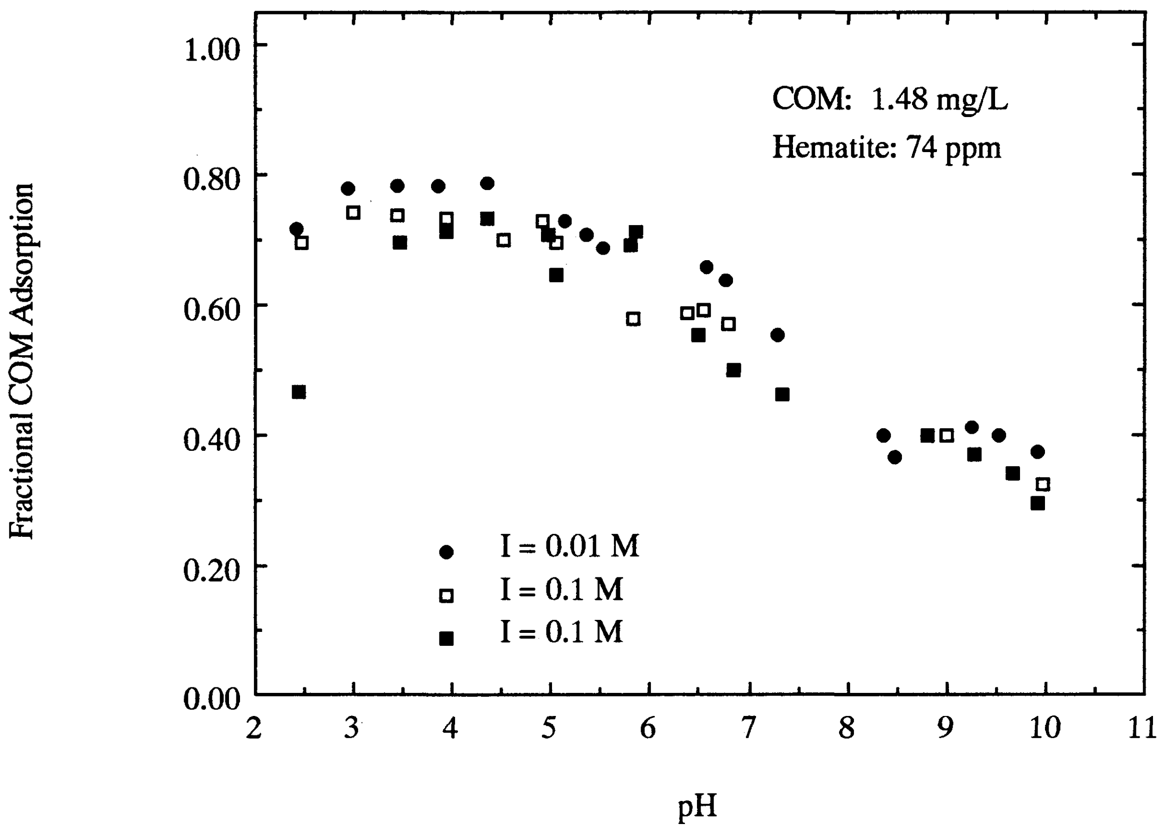

Figure 4.15 Effect of $NaClO_4$ concentration on equilibrium sorption of 1.48 mg/L total COM by 74 ppm hematite (2.73×10^{-6} M).

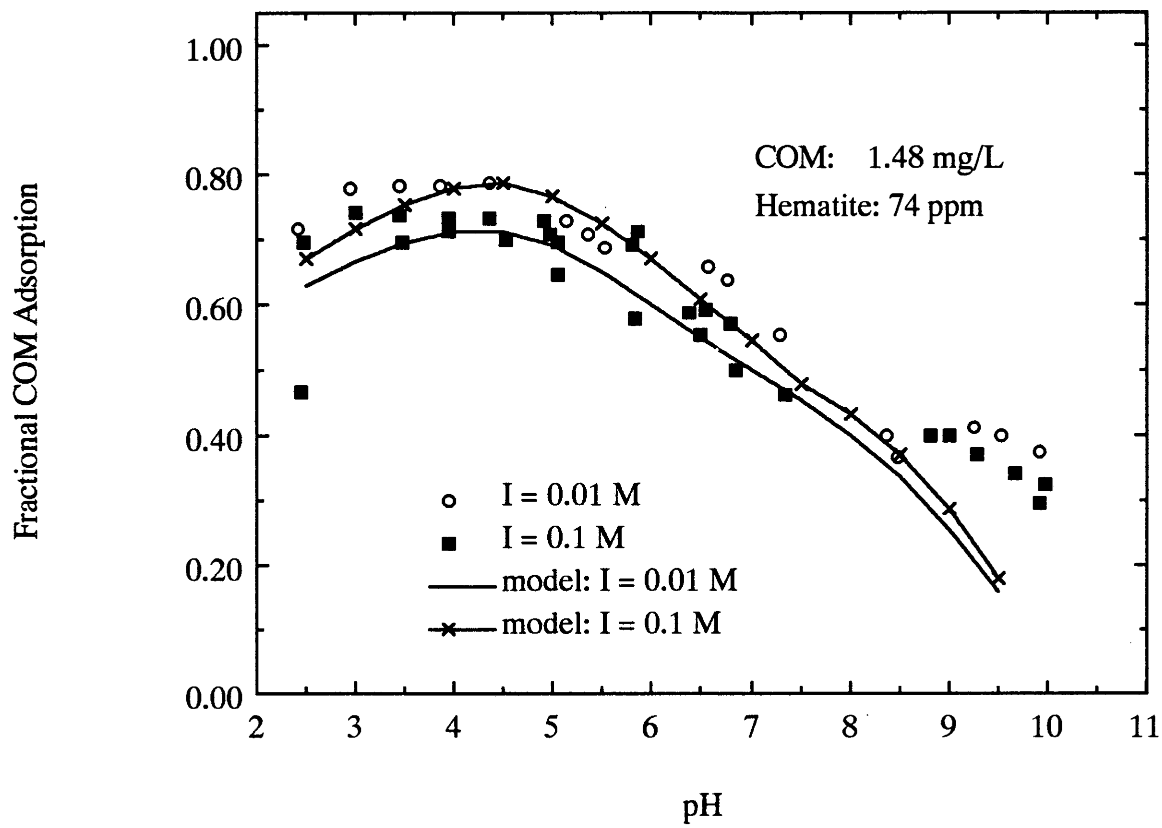

Figure 4.16 Fit of TLM data to experimental data using inner sphere COM complexes for the equilibrium fractional adsorption of 1.48 mg/L total COM by 74 ppm hematite (2.73 x 10^{-6} M) with a background electrolyte concentration of 0.01 and 0.1 M as $NaClO_4$.

4.4 Complexation of Th(IV) by COM

Th(IV) complexation by COM was evaluated over a narrow pH range (pH 2 - 3.5) to avoid complications when separating free Th(IV) from Th-COM complexes at pH values > 3.5. At these higher pH values, an unidentified third phase became visible at the organic/ aqueous phase interface during the separation procedure. The nature and composition of this phase was unknown; therefore, experiments were limited to the pH values discussed above. The extent of Th(IV) complexation was evaluated after 1 hour as complexation rate studies (Cacheris and Choppin, 1987) indicate that at least 95% complexation with humic materials occurs within one minute. Preliminary results demonstrating Th(IV) complexation by COM as a function of pH is presented in Table 4.1. Stability constants from the literature (Martell and Smith, 1977) for Th(IV) complexation with several acid ligands are provided in Table 4.2 for comparison with experimental results. Because our experimental data is for low pH values (below the first COM pK_a of 4.8), ligands for comparison were selected that had pK_a's of ~ 4.8. Calculated results indicate that Th(IV) complexation by COM is greater than that with individual mono- and diprotic acid ligands. This is probably due to the heterogeneity of functional groups in the COM, which would increase its capacity to complex Th(IV).

Table 4.1 Th(IV) complexation by COM as a function of pH for 4 x 10^{-15} M Th(IV) and 1.48 mg/L COM. Reaction stoichiometry assumes H_3COM is a neutral species.

pH	log $K_{Th/COM}$ (l/moles sites)	Fraction Th complexed
2.5	3.75	0.78
3.0	**3.24**	**0.77**
3.5	2.73	0.78

$$Th^{+4} + H_3COM = ThH_2COM^{+3} + H^+ \qquad K_{Th/COM} = \frac{[ThH_2COM^{+3}][H^+]}{[Th^{+4}][H_3COM]}$$

Table 4.2 Comparison of literature stability constants for several acid ligands at pH 3. Values derived from Martell and Smith (1977). Reaction stoichiometry is for a monoprotic acid ligand.

Ligand	pK_a	Structure	log $K_{Th/L}$ (l/moles sites)
Acetic acid	4.8	CH_3COOH	-0.91
Propionic acid	4.67	CH_3CH_2COOH	-0.73
Butyric acid	4.62	$CH_2(CH_2)_2COOH$	-0.72
Isobutyric acid	4.64	$(CH_3)_2CH_2COOH$	-0.79
Malonic acid	5.07	$CH_2(COOH)_2$	2.35
Phthalic acid	4.71	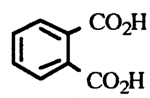	1.21
COM	**4.8**		**3.24**

$$Th^{+4} + HL = ThL^{+3} + H^+ \qquad K_{Th/L} = \frac{[ThL^{+3}][H^+]}{[Th^{+4}][HL]}$$

Comparison of experimental values with those determined from *in situ* samples are provided in Table 4.3. Calculated experimental values compare very well with those from the field, especially those of Santschi *et al.* (1994). The COM used in laboratory experiments was from this *in situ* source.

Table 4.3 Comparison of Th/COM partitioning coefficients.

Location	MW fraction	log K_c (l/kg)	Reference
Gulf of Mexico Lab study pH: 2.5	1 KD - 0.4 μm	**6.23**	This study
Gulf of Mexico Lab study pH: 3.0	1 KD - 0.4 μm	**6.24**	This study
Gulf of Mexico Lab study pH: 3.5	1 KD - 0.4 μm	**6.23**	This study
Gulf of Mexico: field	1 KD - 0.4 μm 10 KD - 0.4 μm	**6.1 ± 0.3** 5.8 - 6.6	Santschi *et al.* (1994) Baskaran *et al.* (1992)
Buzzard's Bay, MA Gulf of Maine	10 KD - 0.2 μm	4.8 - 5.5	Moran and Buessler (1993)
Texas Bays and Estuaries	10 KD - 0.4 μm	4.0 - 5.9	Baskaran and Santschi (1993)

$$K_c = [\text{Th-COM}]/[\text{Th}][\text{COM}]$$

In addition to comparison with literature stability constants and field partitioning values, the HYDRAQL modeling program (Papelis *et al.*, 1988) was used to predict the solution complexation of Th(IV) with COM using the single solution-phase reaction appropriate for the pH range of the experimental data. The reaction stoichiometry used was:

$$Th^{+4} + H_3COM = ThH_2COM + H^+$$

and modeling results shown in Figure 4.17. Model results indicate that Th(IV) interacts with COM predominantly at low pH values and that complexation falls off drastically after pH ~4.5. These results illustrate the inability of the postulated complexation reaction to compete against thorium hydroxy species formation at higher pH values; however, for the experimental pH values examined (pH 2 - 3.5), the model prediction agrees fairly well with the experimental data.

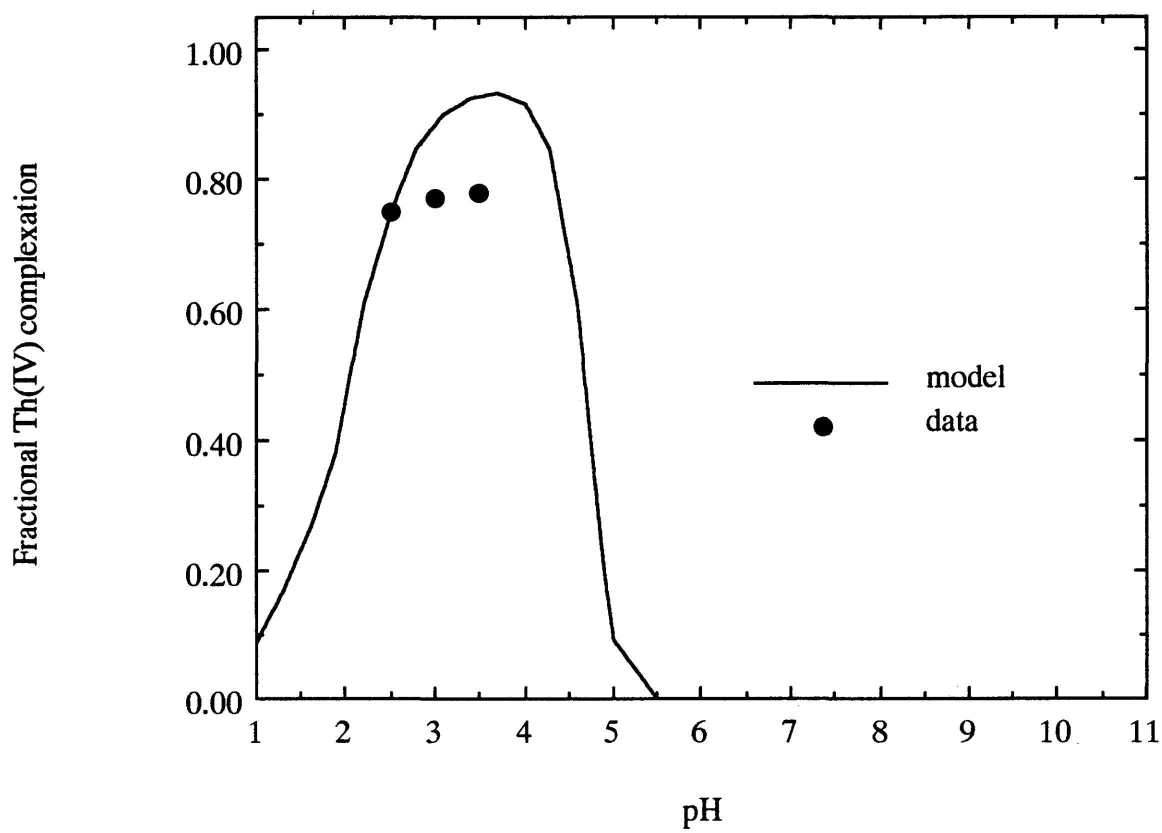

Figure 4.17 TLM simulation of Th(IV) complexation with COM for 4 x 10^{-15} M total Th(IV) and 1.48 mg/L COM with a background electrolyte concentration of 0.01 M as $NaClO_4$.

4.5 Adsorption of Th(IV) by hematite in the presence of COM

Several interactions between system components are possible in a ternary system composed of hematite, Th(IV) and COM. For example, Th(IV) and COM can interact directly with the hematite surface and/or be complexed in solution. Solution phase Th-COM complexes can remain in solution or be surface active. Soluble Th-COM complexes decrease the free Th(IV) concentration over that of ligand-free systems, causing a shift in the observed sorption edge to higher pH values. Surface active Th-COM complexes can enhance or inhibit Th(IV) sorption compared to ligand-free systems depending on factors such as the pH and sorbate/sorbent ratio examined and general solution conditions. It is experimentally difficult to distinguish between Th(IV) and Th-COM complex sorption on the hematite surface; however, observing changes in Th(IV) and COM sorption by hematite in the ternary system allows some conclusions to be drawn about the identity of the surface species.

The effect of COM on Th(IV) fractional adsorption as a function of pH is shown in Figure 4.18. In the presence of COM, Th(IV) adsorption is enhanced at low pH's over that when COM is absent, and is not affected at high pH's. This shift of the sorption edge to lower pH values has been reported by Righetto *et al.*, (1991) for plutonium, americium and neptunium sorption on silica and alumina in the presence of humic acids. Davis (1984) also observed this behavior for copper sorption on alumina in the presence of natural organic matter. Table 4.4 summarizes the results of several studies investigating the effect of natural and synthetic organic ligands on solute sorption. The studies conducted at ambient pH show decreased solute sorption over that in ligand-free systems in contrast to the enhanced sorption reported for solute sorption in variable pH systems. The observed decrease in sorption may be a function of the pH examined and/or the organic ligand concentration, as it has been demonstrated that metal-like sorption behavior can be transformed to ligand-like behavior by increasing the concentration of organic matter in the system (Davis, 1984; Righetto *et al.*, 1991).

Enhanced Th(IV) adsorption in the presence of COM has several possible explanations including: 1) binding of surface active metal/ligand complexes, 2) surface regulation effects (Prieve and Ruckenstein, 1976), 3) uncoiling of COM structure as it approaches the hematite surface exposing new sites, and 4) effect of COM on hematite Ψ_o

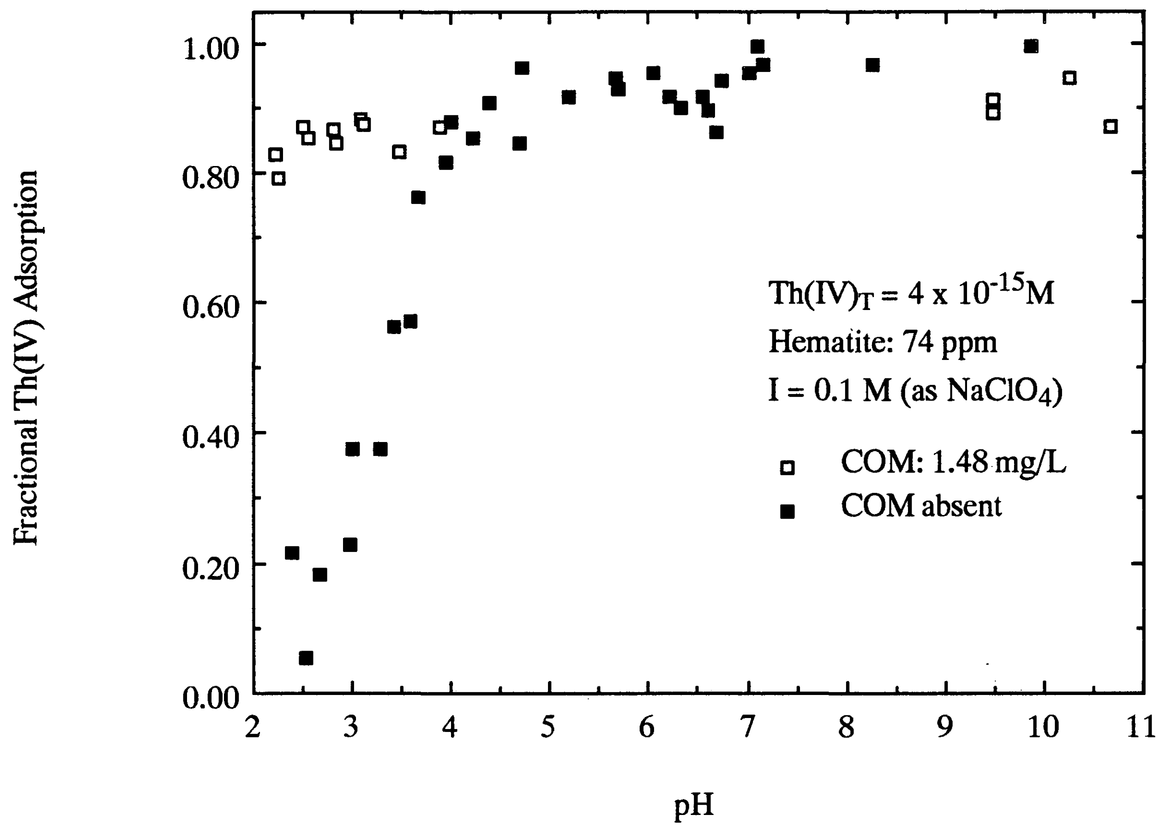

Figure 4.18 Equilibrium fractional Th(IV) sorption edge for 4 x 10^{-15} M total Th(IV), 74 ppm hematite (2.73 x 10^{-6} M) and 1.48 mg/L COM with a background electrolyte concentration of 0.1 M as $NaClO_4$.

Table 4.4 Summary of the effect of natural and synthetic organic ligands on solute sorption.

System (sorbate/ligand/sorbent)	Variable or ambient pH	Results	Source
natural organic matter			
Cu(II)/ ***surface sediment***/silica	variable	Enhanced Cu(II) sorption on silica	Davis, 1984
Am(III), Np(V), Pu/***humic acid***/ alumina	variable	Enhanced Am(III), Np(V), Pu sorption on alumina	Righetto *et al.*, 1991
synthetic organic ligand			
Cu(II)/***2,2' Bipyridil***/silica	variable	Enhanced Cu(II) sorption on silica	Bourg *et al.*, 1979
Np (V)/***EDTA***/hematite	variable	Enhanced Np(V) sorption on hematite	Kohler, *et al.*, 1994
natural organic matter			
Pu(III,IV)/***lake colloids***/lake sediments	ambient	Reduced Pu(III,IV) sorption to suspended sediment particles	Nelson *et al.*, 1985
Th(IV)/***diatom exudates***/alumina	ambient	Reduced Th(IV) sorption on alumina	Niven & Moore, 1987

and σ_0. Additional information is gained in examining COM fractional sorption in the ternary system as a function of pH (Figure 4.19). COM adsorption is unaffected by the presence of Th(IV) in the ternary system which suggests that COM controls sorption in the ternary system, not Th(IV) or surface-active Th-COM complexes. The effects of variation in ionic strength on Th(IV) fractional adsorption in the ternary system is illustrated in Figure 4.20. Once again, sorption appears to be relatively insensitive to changes in ionic strength, which suggests inner-sphere (o - plane) complex formation.

Experimental results were modeled (TLM) treating all system components as previously described. The results of modeling Th(IV) sorption on hematite in the presence of COM as an inner-sphere complex are illustrated in Figure 4.21. While the model overpredicts the effect of COM on Th(IV) sorption when compared to the experimental data, the overall effect, i.e., shifting the sorption edge to lower pH values, was quite similar to that observed. Interestingly, when the complexation reaction for Th(IV) and COM was removed from the model, no effect was seen in the predicted sorption edge. This indicates that Th(IV)/COM interactions are not the cause of enhanced Th(IV) sorption on hematite at low pH's.

Analysis of the hematite surface charge and potential (TLM) in the ternary system showed that sorbed COM decreases (makes less positive) both surface charge and potential over COM-free systems (Figure 4.22). My explanation for enhanced Th(IV) sorption at low pH values, therefore, is that the COM sorbed on the hematite surface changes the surface charge and potential sufficiently to promote Th(IV) sorption at low pH's, even though Th(IV) binds as an inner-sphere complex.

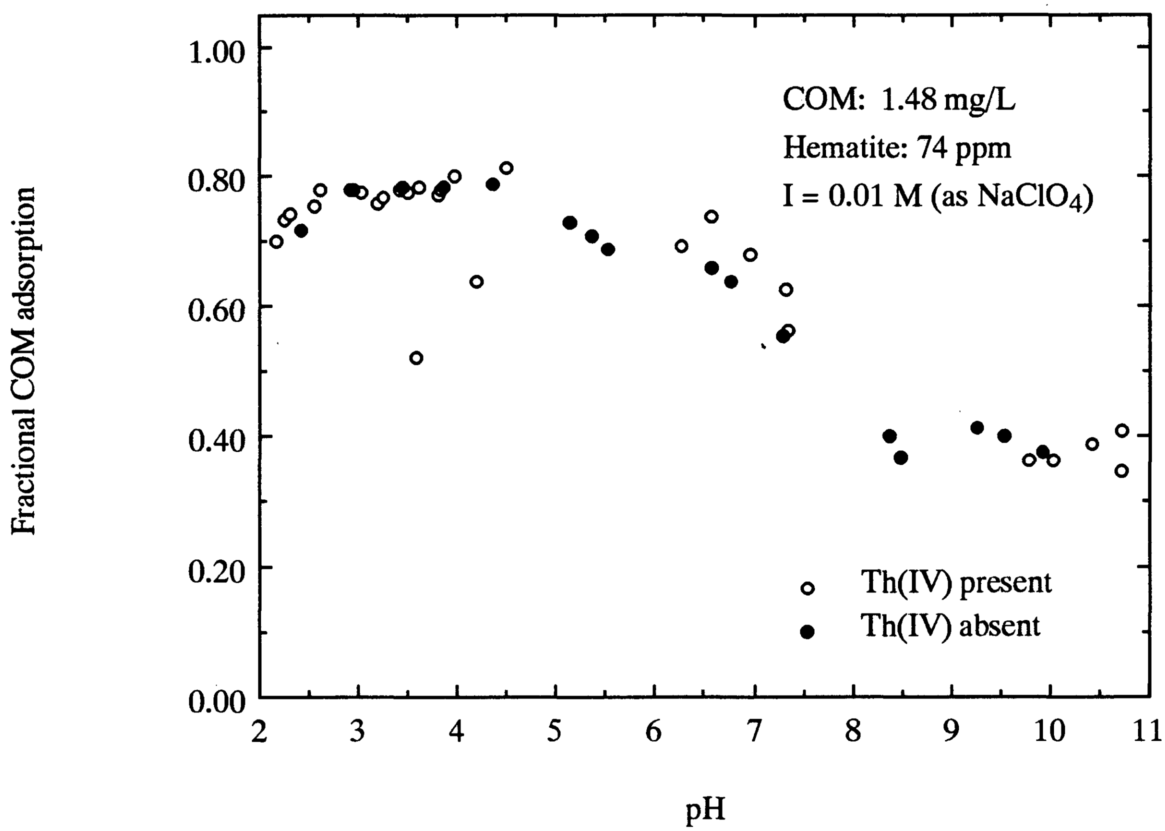

Figure 4.19 Equilibrium fractional COM sorption edge for 1.48 mg/L COM, 74 ppm hematite (2.73×10^{-6} M) and 4×10^{-15} M total Th(IV), with a background electrolyte concentration of 0.01 M as $NaClO_4$.

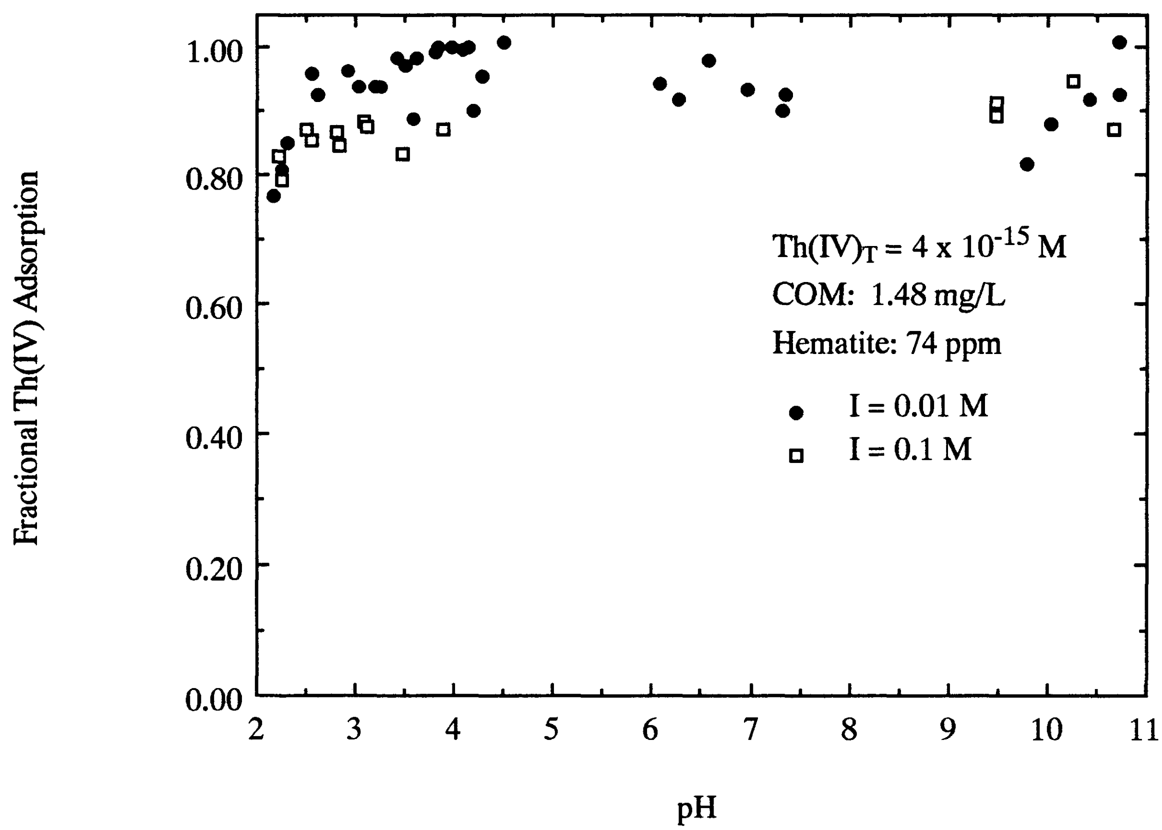

Figure 4.20 Effect of $NaClO_4$ concentration on equilibrium sorption of 4 x 10^{-15} M total Th(IV) by 74 ppm hematite (2.73 x 10^{-6} M) in the presence of 1.48 mg/L COM.

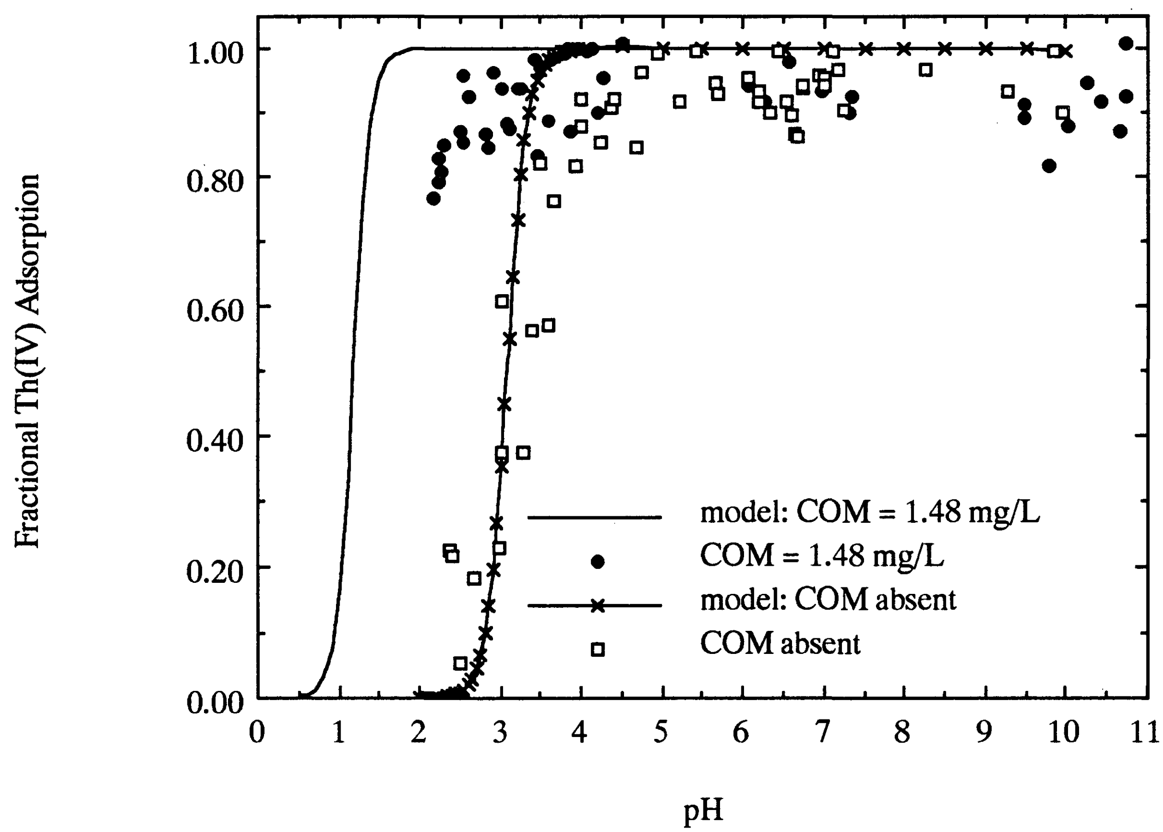

Figure 4.21 Fit of TLM data to experimental data using inner sphere Th(IV) complex formation for 4×10^{-15} M total Th(IV), 74 ppm hematite (2.73×10^{-6} M) in the presence of 1.48 mg/L COM. Data shown for background electrolyte concentration of both 0.01 and 0.1 M as $NaClO_4$.

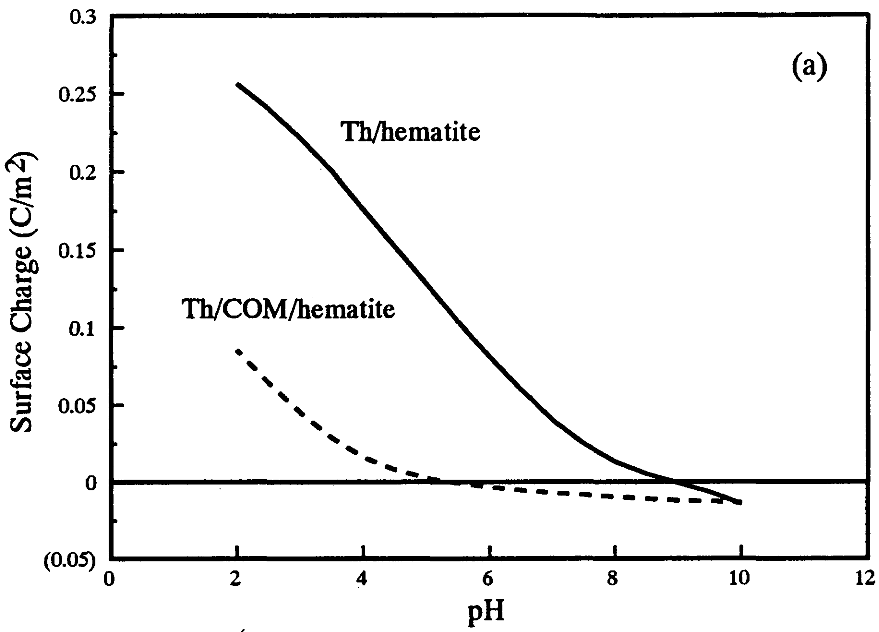

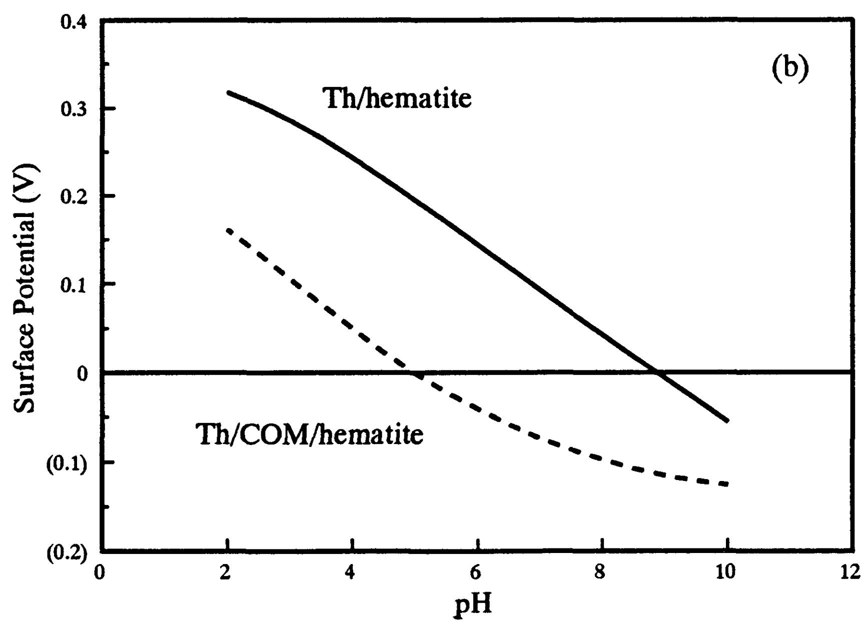

Figure 4.22 Effect of adsorbed COM on hematite surface charge (a), and potential (b).

Chapter 5

CONCLUSIONS

The objective of this laboratory study was to investigate the effect of marine colloidal organic matter (COM) on Th(IV) adsorption in hematite (α-Fe_2O_3) suspensions. Important conclusions based on the results of this study can be summarized as follows:

1. Thorium sorption on hematite occurs as an inner-sphere (coordination) complex. Experimental data can be modeled with one thorium sorbing species (Th^{+4}) using the following reaction stoichiometry:

$$SOH + Th^{+4} = SOTh^{+3} + H^{+} \qquad K^{*}_{int} = \frac{[SOTh][H+]}{[SOH][Th+4]} \exp\left\{\frac{3F\Psi_o}{RT}\right\}$$

$$\log K^{*}_{int} = 17.3$$

2. COM sorption on hematite occurs as an inner-sphere (coordination) complex. Experimental data can be modeled treating the COM as a triprotic acid ligand, with pKa's of 4.8, 7.1 and 9.6 using the following reaction stoichiometries:

$$SOH + H^{+} + COM^{-3} = SOH_2COM^{-2} \qquad \log K^{*}_{int} = 19.2$$

$$SOH + 2H^{+} + COM^{-3} = SOH_2COMH^{-1} \qquad \log \beta^{*}_{2,\,int} = 24.6$$

$$SOH + 3H^{+} + COM^{-3} = SOH_2COMH_2 \qquad \log \beta^{*}_{3,\,int} = 29.1$$

3. Thorium appears to bind to COM more strongly than expected from component acid ligands.

4. Field K_c values must be reconciled with COM functional group information: e.g., competition with hydroxy species at high pH values.

5. Thorium sorption on hematite in the presence of COM occurs as an inner-sphere (coordination) complex.

6. Some Th/COM complexes are not surface active.

7. Thorium sorption on hematite is enhanced in the presence of COM at low pH values. Enhanced binding is not due to surface-active Th/COM complexes.

Additional research in this area should include positive identification of the COM functional groups involved in Th(IV) complexation, and evaluation of Th/COM complexation versus thorium hydroxy species formation at mid to high pH values. Also, clarifying the role sorbed COM plays on hematite surface charge would further our understanding of enhanced Th(IV) sorption on hematite at low pH's in the presence of COM.

REFERENCES

Aleixo, L. M., O. E. S. Godinho and W. F. daCosta. 1992. Potentiometric study of acid-base properties of humic acid using linear functions for treatment of titration data. Analytica Chemica Acta 257: 35-39.

Baes, C. F., Jr., and R. E. Mesmer. 1976. The hydrolysis of cations. New York: John Wiley.

Balistrieri, L. S., P. G. Brewer, and J. W. Murray. 1981. Scavenging residence times of trace metals and surface chemistry of sinking particles in the deep ocean. Deep Sea Research 28: 101-121.

Baskaran, M., P. H. Santschi, G. Benoit, and B. D. Honeyman. 1992. Scavenging of thorium isotopes by colloids in seawater of the Gulf of Mexico. Geochimica et Cosmochimica Acta 56: 3375-3388.

Benjamin, M. M. and J. O. Leckie. 1981. Conceptual model for metal-ligand-surface interactions during adsorption. Environmental Science and Technology 15: 1050-1057.

Benner, R., Pakulski, J. D., McCarthy, M., Hedges, J., and P. Hatcher. 1992. Bulk chemical characteristics of dissolved organic matter in the ocean. Science 255: 1561-1564.

Bhat, S. G., S. Krishnaswami, D. Lal and W. S. Moore. 1969. Th^{234}/U^{238} ratios in the ocean. Earth and Planetary Science Letters 5: 483-491.

Breeuwsma, A. 1973. Adsorption of ions on hematite. Ph.D. dissertation, Agricultural University, Wageningen, The Netherlands.

Broecker, W. S., A. Kaufman and R. M. Trier. 1973. The residence time of thorium in surface sea water and its implications regarding the rate of reactive pollutants. Earth and Planetary Science Letters 20: 35-44.

Buffle, J., R. S. Altmann, M. Filella and A. Tessier. 1990. Complexation by natural heterogeneous compounds: Site occupation distribution functions, a normalized description of metal complexation. Geochimica et Cosmochimica Acta 54: 1535-1553.

Cacheris, W. P. and G. R. Choppin. 1987. Dissociation kinetics of thorium-humate-complex. Radiochimica Acta 42: 185-190.

Choppin, G. R. and L. Kullberg. 1978. Protonation thermodynamics of humic acid. Journal of Inorganic Nuclear Chemistry 40: 651-654.

Davis, J. A. 1982. Adsorption of natural dissolved organic matter at the oxide/water interface. Geochimica et Cosmochimica Acta 46: 2381-2393.

Davis, J. A. 1984. Complexation of trace metals by adsorbed natural organic matter. Geochimica et Cosmochimica Acta 48: 679-691.

Davis, J. A. and D. B. Kent. 1990. Surface complexation modeling in aqueous geochemistry. Reviews in Mineralogy, vol. 23. M. F. Hochella, Jr., and A. F. White (eds.). Washington, D. C.: Mineralogy Society of America.

Davis, J. A., R. O. James and J. O. Leckie. 1978. Surface ionization and complexation at the oxide/water interface: (I) computation of electrical double layer properties in simple electrolytes. Journal of Colloid and Interface Science 63 (3): 480-499.

Dzombak and Morel. 1990. Surface complexation modeling: hydrous ferric oxides. New York: John Wiley and Sons, Inc.

Gamble, D. S. 1970. Titration curves of fulvic acid: the analytical chemistry of a weak acid polyelectrolyte. Canadian Journal of Chemistry 48: 2662-2669.

Goldberg, E. D. 1954. Marine Geochemistry. I. Scavengers of the sea. Journal of Geology 62; 249-265.

Guo, L., C. H. Coleman Jr. and P. H. Santschi. 1993. The distribution of colloidal and dissolved organic carbon in the Gulf of Mexico. Marine Chemistry 44: 1-15.

Hayes, K. F. and J. O. Leckie. 1987. Modeling ionic strength effects on cation adsorption at hydrous oxide/solution interfaces. Journal of Colloid and Interface Science 115: 564-572.

Hayes, K. F., C. Papelis, and J. O. Leckie. 1988. Modeling ionic strength effects on anion adsorption at hydrous oxide/solution interfaces. Journal of Colloid and Interface Science 125 (2): 717-726.

Honeyman, B. D., L. S. Balistrieri and J. W. Murray. 1988. Oceanic trace metal scavenging: the importance of particle concentration. Deep-Sea Research 35 (2): 227-246.

Honeyman, B. D. and P. H. Santschi. 1989. A Brownian-pumping model for oceanic trace metal scavenging: evidence from Th isotopes. Journal of Marine Research 47: 951-952.

Honeyman, B. D. 1991. Surface chemistry, colloids and trace element scavenging. Marine Particles: Analysis and Characterization, Geophysical Monograph 63: 437-451.

Honeyman, B. D. and P. H. Santschi. 1991. Coupling adsorption and particle aggregation: laboratory studies of "colloidal pumping" using ^{59}Fe-labeled hematite. Environmental Science and Technology 25 (10): 1739-1747.

Honeyman, B. and P. Santschi. 1992. The role of particles and colloids in the transport of radionuclides and trace metals in the oceans. Environmental Particles. Jacques Buffle and Herman P. van Leeuwen (eds.). London: Lewis Publishers.

Hunter, K. A., D. J. Hawke and L. K. Choo. 1988. Equilibrium adsorption of thorium by metal oxides in marine electrolytes. Geochimica et Cosmochimica Acta 52: 627-636.

Jannasch, H. W., B. D. Honeyman, L. S. Balistrieri, and J. W. Murray. 1988. Kinetics of trace element uptake by marine particles. Geochimica et Cosmochimica Acta 52: 567-577.

Kohler, M., B. D. Honeyman and J. O. Leckie. 1992. Np (V) adsorption on hematite in aqueous suspension: effects of carbonate and EDTA. Submitted to Geochimica et Cosmochimica Acta.

Koike, I., S. Hara, K. Terauchi and K. Kogure. 1990. Role of sub-micrometer particles in the ocean. Nature 345: 242-243.

LaFlamme, B. D., and J. W. Murray. 1987. Solid/solution interaction: the effect of carbonate alkalinity on adsorbed thorium. Geochimica et Cosmochimica Acta 51: 243-250.

Langmuir, D. and J. S. Herman. 1980. The mobility of thorium in natural waters at low temperatures. Geochimica et Cosmochimica Acta 44: 1753-1766.

Li, Y.-H., L. Burkhardt, M. Buccholtz, P. O'Hara, and P. H. Santschi. 1984. Partition of radiotracers between suspended particles and seawater. Geochimica et Cosmochimica Acta 48: 2011-2019.

Liang, L. 1988. Effects of surface chemistry on kinetics of coagulation of submicron iron oxide particles in water. Ph.D. dissertation, California Institute of Technology, San Diego, California.

Longhurst, A. R., I. Koike, W. K. W. Li, J. Rodriguez, P. Dickie, P. Kepay, F. Partensky, B. Bautista, J. Ruiz, M. Wells and D. F. Bird. 1992. Sub-micron particles in northwest Atlantic shelf water. Deep-Sea Research. 39: 1-7.

Manunza, B., C. Gessa, S. Deiana and R Rausa. 1992. A normal distribution model for the titration curves of humic acids. Journal of Soil Science 43: 127-131.

Martell, A. E. and R. M. Smith. 1977. Critical stability constants, vol. 3. New York: Plenum Press.

Matijevic, E. and P. Scheiner. 1978. Ferric hydrous oxide sols. Journal of Colloid and Interface Science 63 (3): 509.

Moore, R. M. and K. A. Hunter. 1985. Thorium adsorption in the ocean: reversibility and distribution amongst particle sizes. Geochimica et Cosmochimica Acta 49: 2253-2257.

Moore, R. M. and G. E. Millward. 1988. The kinetics of reversible Th reactions with marine particles. Geochimica et Cosmochimica Acta 52: 113-118.

Moore, W. S. and W. M. Sackett. 1964. Uranium and thorium series inequilibrium in seawater. Journal of Geophysical Research 69: 5401-5405.

Moore, W. S. 1969. Measurement of Ra^{228} and Th^{228} in seawater. Journal of Geophysical Research 74: 694.

Moran, S. B. and R. M. Moore. 1989. The distribution of colloidal aluminum and organic carbon in coastal and open ocean water off Nova Scotia. Geochimica et Cosmochimica Acta 53: 2519-2527.

Moran, S. B. and R. M. Moore. 1992. Kinetics of the removal of dissolved aluminum by diatoms in seawater: A comparison with thorium. Geochimica et Cosmochimica Acta 56: 0001-0010.

Moran, S. B. and K. O. Buesseler. 1993. Size fractionated 234Th in continental shelf waters off New England: implications for the role of colloids in oceanic trace metal scavenging. Submitted to Journal of Marine Research.

Morel, F. M. M. and P. M. Gschwend. 1987. The role of colloids in the partitioning of solutes in natural waters. Aquatic Surface Chemistry: Chemical Processes at the Particle-Water Interface. Werner Stumm (ed.). New York: John Wiley & Sons.

Nash, K. L. and G. Choppin. 1980. Interaction of humic and fulvic acids with Th(IV). Journal of Inorganic Nuclear Chemistry 42: 1045-1050.

Nelson, D. M., W. R. Penrose, John O. Karttunen, and Paige Mehlhaff. 1985. Effects of dissolved organic carbon on the adsorption properties of plutonium in natural waters. Environmental Science and Technology 19(2): 127-131.

Niven, S. E. H. and R. M. Moore. 1987. Effect of natural colloidal matter in the equilibrium adsorption of thorium in seawater. Radionuclides: A Tool for Oceanography. J. C. Guary, P. Gueguenait, and R. J. Pentreath (eds.) New York: Elsevier Science Publishing Co., Inc.

Niven, S. E. H. and R. M. Moore. 1993. Thorium sorption in seawater suspensions of aluminum oxide particles. Geochimica et Cosmochimica Acta 57: 2169-2179.

Niven, S. E. H. 1989. Solid-solution partitioning of thorium in seawater. Ph.D. dissertation, Dalhousie University, Halifax, Nova Scotia.

Nozaki, Y., Y. Horibe and H. Tsubota. 1981. The water column distributions of thorium isotopes in the western North Pacific. Earth and Planetary Science Letters 54: 203-216.

Nyffeler, U. P., Y.-H. Li and P. H. Santschi. 1984. A kinetic approach to describe trace element distribution between particles and solution in natural systems. Geochimica et Cosmochimica Acta 48: 1513-1522.

Quigley, M., B. D. Honeyman and P. H. Santschi. 1994. Laboratory studies of thorium sorption and desorption kinetics. Manuscript in preparation.

Papelis, C., K. F. Hayes, and J. O. Leckie. 1988. HYDRAQL: A program for the computation of chemical equilibrium composition of aqueous batch systems including surface-complexation modeling of ion adsorption at the oxide/solution interface. Department of Civil Engineering, Stanford University, Stanford, California.

Penners, N. H. G. 1985. The preparation and stability of homodisperse colloidal hematite (α-Fe_2O_3). Ph.D. dissertation, Agricultural University, Wageningen, The Netherlands.

Peppard, D. F., G. W. Mason, J. L. Maier and W. J. Driscoll. 1957. Fractional extraction of the lanthanides as their di-alkyl orthophosphates. Journal of Inorganic Nuclear Chemistry 4: 334-343.

Prieve, D. C. and E. Ruckenstein. 1976. The surface potential of and double-layer interaction force between surfaces characterized by multiple ionizable groups. Journal of Theoretical Biology 56: 205-228.

Righetto, L., G. Bidoglio, G. Azimonti and I R. Bellobono. 1991. Competitive actinide interactions in colloidal humic acid-mineral oxide systems. Environmental Science and Technology 25: 1913- 1919.

Santschi, P. H., D. Adler, M. Amdurer, Y. H. Li and J. J. Bell. 1980. Thorium isotopes as analogues for "particle-reactive" pollutants in coastal marine environments. Earth and Planetary Science Letters 47: 327-335.

Santschi, P. H. and B. D. Honeyman. 1991. Are thorium scavenging and particle fluxes in the ocean regulated by coagulation? Radionuclides in the study of marine processes. P. J. Kershaw and D. S. Woodhead (eds.). New York: Elsevier Applied Science.

Schindler, P. W. and W. Stumm. 1987. The surface chemistry of oxides, hydroxides and oxides minerals. Aquatic Surface Chemistry: Chemical Processes at the Particle-Water Interface. Werner Stumm (ed.). New York: John Wiley & Sons.

Shaw, Duncan J. 1991. Introduction to colloid and surface chemistry,. 4th edition. Oxford: Butterworth-Heineman Ltd.

Tipping, E. 1981. The adsorption of aquatic humic substances by iron oxides. Geochimica et Cosmochimica Acta 45: 191-199.

Weber Jr., W. J., P. M. McGinley and L. E. Katz. 1991. Sorption phenomena in subsurface systems: concepts, model and effects on contaminant fate and transport. Water Research 25: 499-528.

Wells, M. L. and E. D. Goldberg. 1991. Occurrence of small colloids in sea water. Nature 353: 342-344.

Wolfinbarger, Lloyd Jr. and Michael P. Crosby. 1983. A convenient procedure for radio-labeling detritus with [^{14}C] dimethylsulfate. Journal of Experimental Marine Biology and Ecology 67: 185-198.

SELECTED BIBLIOGRAPHY

Selected bibliography lists sources of information related to this thesis topic, but not specifically cited in the thesis.

Buesseler, K. O. 1991. Do upper-ocean sediment traps provide an accurate record of particle flux? Nature 353: 420-423.

Comans, R. N. J. and J. J. Middelburg. 1987. Sorption of trace metals on calcite: Applicability of the surface precipitation model. Geochimica et Cosmochimica Acta 51: 2587-2591.

Davis, J. A. and J. O. Leckie. 1978. Surface ionization and complexation at the oxide/water interface: (II) surface properties of amorphous iron oxyhydroxide and adsorption of metal ions. Journal of Colloid and Interface Science 67 (1): 90-107.

Davis, J. A. and J. O. Leckie. 1980. Surface ionization and complexation at the oxide/water interface: (3) adsorption of anions. Journal of Colloid and Interface Science 74 (1): 32-43.

Farley, K. J., D. A. Dzombak and F. M. M. Morel. 1985. A surface precipitation model for the sorption of cations on metal oxides. Journal of Colloid and Interface Science 106 (1): 226-242.

Hayes, K. F., C. Papelis, and J. O. Leckie. 1988. Modeling ionic strength effects on anion adsorption at hydrous oxide/solution interfaces. Journal of Colloid and Interface Science 125 (2): 717-726.

Honeyman, B. D. and J. O. Leckie. 1986. Macroscopic partitioning coefficients for metal ion adsorption - proton stoichiometry at variable pH and adsorption density. ACS Symposium Series 323 - Geochemical Processes at Mineral Surfaces. James A. Davis and Kim F. Hayes, eds.

Honeyman, B. D. 1988. Particle-particle interactions: a new paradigm for aquatic chemists? Applied Geochemistry 3: 77.

James, R. O., J. A. Davis and J. O. Leckie. 1978. Computer simulation of the conductometric and potentiometric titrations of the surface groups on ionizable latexes. Journal of Colloid and Interface Science 65 (2): 331-344.

Leckie, J. O. 1986. Adsorption and transformation of trace element species at sediment/water interfaces. The Importance of Chemical "Speciation" in Environmental Processes. Heidelberg: Dahlem Konferenzen: 237-254.

Persin, P., L. Charlet, R. Karthein, and W. Stumm. 1989. From adsorption to precipitation: Sorption of Mn^{2+} on $FeCO_3(s)$. Geochimica et Cosmochimica Acta 53: 2787-2796.

Santschi, P. H. and B. D. Honeyman. 1989. Radionuclides in aquatic environments. Radiation Physics and Chemistry 34 (2): 213-240.

Sposito, G.. 1992. Characterization of particle surface charge. Environmental Particles. Jacques Buffle and Herman P. van Leeuwen (eds.). London: Lewis Publishers.

Tipping, E. 1986. Some aspects of the interactions between particulate oxides and aquatic humic substances. Marine Chemistry 18: 161-169.

Toggweiler, J. R. 1990. Diving into the organic soup. Nature 345: 203-204.

Westal, J. C. 1987. Adsorption mechanisms in aquatic surface chemistry. Aquatic Surface Chemistry: Chemical Processes at the Particle-Water Interface. Werner Stumm (ed.). New York: John Wiley & Sons.

APPENDIX A

Thorium (IV) Adsorption by Hematite - Experimental Data

Table A-1. Experimental adsorption data for 4 x 10^{-15} M total Th(IV), 74 ppm hematite (2.73 x 10^{-6} M) and 0.1 M total background electrolyte concentration as $NaClO_4$ (Figure 4.8).

pH	Fractional adsorption
2.515	0.0527
3.003	0.3752
3.401	0.5610
3.652	0.7623
3.985	0.8807
4.382	0.9072
4.725	0.9621
5.196	0.9161
5.683	0.9301
6.200	0.9177
6.543	0.9173
6.684	0.8636
7.100	0.9969
7.16	0.9678
8.266	0.9651
9.852	0.9941

Table A-2. Experimental adsorption data for 4 x 10^{-15} M total Th(IV), 74 ppm hematite (2.73 x 10^{-6} M) and 0.1 M total background electrolyte concentration as $NaClO_4$ (Figure 4.8).

pH	Fractional adsorption
2.388	0.2179
2.661	0.1841
2.979	0.2294
3.273	0.3767
3.583	0.5707
3.935	0.8168
4.222	0.8551
4.683	0.8462
5.651	0.9477
6.052	0.9525
6.315	0.8988
6.606	0.896
6.739	0.9437
7.014	0.9534

Table A-3. Experimental adsorption data for 4 x 10^{-15} M total Th(IV), 74 ppm hematite (2.73 x 10^{-6} M) and 0.01 M total background electrolyte concentration as $NaClO_4$ (Figure 4.9).

pH	Fractional adsorption
2.364	0.2243
3.027	0.6092
3.478	0.8205
3.993	0.9217
4.405	0.9198
4.956	0.9899
5.412	0.9969
6.206	0.9351
6.445	0.9967
6.619	0.8673
6.720	0.9382
6.949	0.9581
7.020	0.9405
7.248	0.9037
9.268	0.9331
9.951	0.8985

APPENDIX B

Marine Colloidal Organic Matter Adsorption by Hematite - Experimental Data

Table B-1. Experimental adsorption data for 1.48 mg/L COM, 74 ppm hematite (2.73×10^{-6} M) and 0.1 M total background electrolyte concentration as $NaClO_4$ (Figure 4.14).

pH	Fractional adsorption
2.475	0.6967
3.003	0.7427
3.449	0.7368
3.928	0.7320
4.522	0.7006
4.907	0.7288
5.043	0.6978
5.819	0.5802
6.365	0.5863
6.528	0.5924
6.783	0.5716
8.997	0.4016
9.962	0.3257

Table B-2. Experimental adsorption data for 1.48 mg/L COM, 74 ppm hematite (2.73×10^{-6} M) and 0.1 M total background electrolyte concentration as $NaClO_4$ (Figure 4.14).

pH	Fractional adsorption
2.439	0.4646
3.460	0.6967
3.933	0.7114
4.355	0.7316
4.974	0.7086
5.045	0.6455
5.802	0.6906
5.855	0.7127
6.475	0.5543
6.835	0.5005
7.346	0.4606
8.805	0.3985
9.296	0.3709
9.676	0.3396
9.930	0.2943

Table B-3. Experimental adsorption data for 1.48 mg/L COM, 74 ppm hematite (2.73×10^{-6} M) and 0.01 M total background electrolyte concentration as $NaClO_4$ (Figure 4.15).

pH	Fractional adsorption
2.404	0.7179
2.943	0.7772
3.430	0.7834
3.861	0.7824
4.364	0.7856
5.127	0.7310
5.348	0.7073
5.517	0.6879
6.557	0.6581
6.767	0.6387
7.277	0.5549
8.380	0.4015
8.476	0.3654
9.253	0.4123
9.546	0.4007
9.923	0.3759

APPENDIX C

Thorium (IV) Adsorption by Hematite in the presence of
Marine Colloidal Organic Matter- Experimental Data

Table C-1. Experimental adsorption data for 4 x 10^{-15} M total Th(IV), 74 ppm hematite (2.73 x 10^{-6} M), 1.48 mg/L COM, and 0.1 M total background electrolyte concentration as $NaClO_4$ (Figure 4.18).

pH	Fractional adsorption
2.247	0.7916
2.549	0.8556
2.840	0.8464
3.106	0.8770
3.468	0.8338
3.870	0.8724
9.480	0.8908
10.658	0.8712

Table C-2. Experimental adsorption data for 4 x 10^{-15} M total Th(IV), 74 ppm hematite (2.73 x 10^{-6} M), 1.48 mg/L COM, and 0.1 M total background electrolyte concentration as $NaClO_4$ (Figure 4.18).

pH	Fractional adsorption
2.231	0.8290
2.511	0.8727
2.794	0.8647
3.085	0.8815
9.468	0.9120
10.260	0.9442

Table C-3. Experimental adsorption data for 4 x 10^{-15} M total Th(IV), 74 ppm hematite (2.73 x 10^{-6} M), 1.48 mg/L COM, and 0.01 M total background electrolyte concentration as $NaClO_4$ (Figure 4.20).

pH	Fractional adsorption
2.305	0.8513
2.554	0.9569
2.923	0.9636
3.233	0.9369
3.415	0.9831
3.496	0.9693
3.791	0.9925
3.832	1.000
3.966	1.000
4.488	1.010
6.255	0.9150
6.581	0.9809
6.963	0.9342
7.309	0.8989
7.345	0.9242
10.735	1.0010

Table C-4. Experimental adsorption data for 4 x 10^{-15} M total Th(IV), 74 ppm hematite (2.73 x 10^{-6} M), 1.48 mg/L COM, and 0.01 M total background electrolyte concentration as $NaClO_4$ (Figure 4.20).

pH	Fractional adsorption
2.165	0.7678
2.261	0.8091
2.599	0.9234
3.017	0.9378
3.204	0.9358
3.588	0.8895
3.605	0.9828
4.075	0.9968
4.144	1.000
4.201	0.9011
4.28	0.9549
6.057	0.9419
9.775	0.8166
10.027	0.881
10.431	0.9176
10.723	0.9235

APPENDIX D

^3H Marine Colloidal Organic Matter (COM) Adsorption by Hematite in the presence of Thorium (IV) - Experimental Data

Table D-1. Experimental adsorption data for 1.48 mg/L COM, 4 x 10^{-15} M total Th(IV), 74 ppm hematite (2.73 x 10^{-6} M), and 0.01 M total background electrolyte concentration as $NaClO_4$ (Figure 4.19).

pH	Fractional adsorption
2.305	0.7400
2.554	0.7562
2.923	0.7797
3.233	0.7657
3.415	0.7807
3.496	0.7746
3.791	0.7705
3.832	0.7792
3.966	0.8004
4.488	0.8140
6.255	0.6907
6.581	0.7380
6.963	0.6811
7.309	0.6260
7.345	0.5612
10.735	0.4085

Table D-2. Experimental adsorption data for 1.48 mg/L COM, 4 x 10^{-15} M total Th(IV), 74 ppm hematite (2.73 x 10^{-6} M), and 0.01 M total background electrolyte concentration as $NaClO_4$ (Figure 4.19).

pH	Fractional adsorption
2.165	0.6991
2.261	0.7320
2.599	0.7805
3.017	0.7747
3.204	0.7563
3.588	0.5203
3.605	0.7838
4.201	0.6371
9.775	0.3618
10.027	0.3636
10.431	0.3871
10.723	0.3470

Table D-3. Experimental adsorption data for 1.48 mg/L COM, 74 ppm hematite (2.73×10^{-6} M), and 0.01 M total background electrolyte concentration as $NaClO_4$ (Figure 4.19).

pH	Fractional adsorption
2.404	0.7179
2.943	0.7772
3.430	0.7834
3.861	0.7824
4.364	0.7856
5.127	0.731
5.348	0.7073
5.517	0.6879
6.557	0.6581
6.767	0.6387
7.277	0.5549
8.380	0.4015
8.476	0.3654
9.253	0.4123
9.546	0.4007
9.923	0.3759

APPENDIX E

Modeling Data: HYDRAQL Input File

Figure E-1. Input screen for model simulation of Th(IV) adsorption on hematite using five outer-sphere thorium species for 4 x 10^{-15} M Th(IV), 74 ppm hematite (2.73 x 10^{-6} M), and 0.1 M total background electrolyte concentration as $NaClO_4$.

```
Adsorption of Th(IV) on hematite; calculations for 120 nm particles 74 ppm
Triple-Layer Model configuration: outer-sphere (b-plane) complexes
0.100   0   0.00   25.00 1.00E-5 1   100   /XMU    KEYMU ACTCOR  TEMP  EPS  NCASES  ITMAX
1    1    1    1    1    1                 /IHYDRA  IINPUT  ICHARG  IPDIST  IPCENT IALLP
1    1    4    0    80000                  /KEY    IADS    MODEL   IDIFOP   LIMADS
1.2   0.2   0    0.706   0   0   0   0     /C11  C21   C31   AREA1  C12   C22   C32   AREA2
31  50  86110   86105   86140   86130   86120  0  0  0  0  0  0  0  0  0  0  0  0  0/
2.0    10.0    0.1                         /line for pH stepping
174          -2.000    1.000E-1            /components          ClO4-
50           -4.000    0.0                 /                    H+
5            -2.000    1.000E-1            /                    Na+
31           -18.000   4.000E-15           /                    Th+4
184          -6.000    2.73100E-6          /                    SOH
180          -1        0.000               /                    PSIO
182          -1        0.000               /                    PSIB
183          -1.3      0.000               /                    PSID
0             0.000    0.000               /
2
12090      -3.22     31    1    50    -1    0     0   0    0   0    0   0    0/
38011      -6.94     31    1    50    -2    0     0   0    0   0    0   0    0/
38012      -11.7     31    1    50    -3    0     0   0    0   0    0   0    0/
38013      -15.87    31    1    50    -4    0     0   0    0   0    0   0    0/
86105      -10.3     184   1    50    -1    180  -1   0    0   0    0   0    0/
86110       6.7      184   1    50     1    180   1   0    0   0    0   0    0/
86115      -9.5      184   1    50    -1    180  -1   5    1   182  1   0    0/
86120       7.5      184   1    50     1    180   1   174  1   182 -1   0    0/
86130       3.3      184   1    50    -1    31    1   180 -1   182  4   0    0/
86131      -1.0      184   1    50    -2    31    1   180 -1   182  3   0    0/
86132      -7.0      184   1    50    -3    31    1   180 -1   182  2   0    0/
86133      -10.63    184   1    50    -4    31    1   180 -1   182  1   0    0/
86134      -16.32    184   1    50    -5    31    1   180 -1   0    0   0    0/
0           0        0     0    0      0    0     0   0    0   0    0   0    0/
3                                                                           /
50       4.00  0 0 0 0 0 0 0 0 0 0 0 0 0 0 0 0 0 0 0 0 0 0 0 0 0 0 0 0 0 0 0 /
0        0.00  0 0 0 0 0 0 0 0 0 0 0 0 0 0 0 0 0 0 0 0 0 0 0 0 0 0 0 0 0 0 0 /
6                                                                           /
180      0.00  0 0 0 0 0 0 0 0 0 0 0 0 0 0 0 0 0 0 0 0 0 0 0 0 0 0 0 0 0 0 0 /
182      0.00  0 0 0 0 0 0 0 0 0 0 0 0 0 0 0 0 0 0 0 0 0 0 0 0 0 0 0 0 0 0 0 /
183      0.00  0 0 0 0 0 0 0 0 0 0 0 0 0 0 0 0 0 0 0 0 0 0 0 0 0 0 0 0 0 0 0 /
0  0   0 0 0 0  0 0 0 0 0 0 0 0 0 0 0 0 0 0 0 0 0 0 0 0 0 0 0 0 0 0 0 0 0 0 0 /
0  0   0 0 0 0  0 0 0 0 0 0 0 0 0 0 0 0 0 0 0 0 0 0 0 0 0 0 0 0 0 0 0 0 0 0 0 /
```

Figure E-2. Input screen for model simulation of Th(IV) adsorption on hematite using one inner-sphere thorium hydroxy species for 4 x 10^{-15} M Th(IV), 74 ppm hematite (2.73 x 10^{-6} M), and 0.1 M total background electrolyte concentration as $NaClO_4$.

```
Adsorption of Th(IV) on hematite; calculations for 120 nm particles 74 ppm
Triple-Layer Model configuration: inner-sphere (o-plane) complexes
0.100   0   0.00  25.00 1.00E-5 1   100   /XMU   KEYMU ACTCOR  TEMP   EPS   NCASES   ITMAX
1     1     1     1     1     1           /IHYDRA  IINPUT  ICHARG   IPDIST  IPCENT IALLP
1     1     4     0     80000             /KEY    IADS    MODEL    IDIFOP    LIMADS
1.2   0.2   0     0.706   0   0   0   0   /C11  C21   C31   AREA1  C12   C22   C32   AREA2
31  50  86110   86105   8̀6140   86130   86120  0  0  0  0  0  0  0  0  0  0  0  0  0/
2.0    10.0     0.1                       /line for pH stepping
174            -2.000     1.000E-1        /components          ClO4-
50             -4.000     0.0             /                    H+
5              -2.000     1.000E-1        /                    Na+
31             -18.000    4.000E-15       /                    Th+4
184            -6.000     2.73100E-6      /                    SOH
180            -1         0.000           /                    PSIO
182            -1         0.000           /                    PSIB
183            -1.3       0.000           /                    PSID
0               0.000     0.000           /
2
12090       -3.22        31     1     50     -1     0      0    0    0    0    0    0    0/
38011       -6.94        31     1     50     -2     0      0    0    0    0    0    0    0/
38012       -11.7        31     1     50     -3     0      0    0    0    0    0    0    0/
38013       -15.87       31     1     50     -4     0      0    0    0    0    0    0    0/
86105       -10.3        184    1     50     -1     180   -1    0    0    0    0    0    0/
86110        6.7         184    1     50      1     180    1    0    0    0    0    0    0/
86115       -9.5         184    1     50     -1     180   -1    5    1    182  1    0    0/
86120        7.5         184    1     50      1     180    1    174  1    182 -1    0    0/
86130        17.3        184    1     50     -1     31     1    180  3    0    0    0    0/
86131       -99.0        184    1     50     -2     31     1    180  2    0    0    0    0/
86132       -99.0        184    1     50     -3     31     1    180  1    0    0    0    0/
86133       -99.0        184    1     50     -4     31     1      0 0    0    0    0    0/
86134       -99.0        184    1     50     -5     31     1    180 -1    0    0    0    0/
0            0           0      0     0      0      0      0    0    0    0    0    0    0/
3                                                                                      /
50        4.00  0 0 0 0 0 0 0 0 0 0 0 0 0 0 0 0 0 0 0 0 0 0 0 0 0 0 0 0 0 0 0 /
0         0.00  0 0 0 0 0 0 0 0 0 0 0 0 0 0 0 0 0 0 0 0 0 0 0 0 0 0 0 0 0 0 0 /
6                                                                                      /
180       0.00  0 0 0 0 0 0 0 0 0 0 0 0 0 0 0 0 0 0 0 0 0 0 0 0 0 0 0 0 0 0 0 /
182       0.00  0 0 0 0 0 0 0 0 0 0 0 0 0 0 0 0 0 0 0 0 0 0 0 0 0 0 0 0 0 0 0 /
183       0.00  0 0 0 0 0 0 0 0 0 0 0 0 0 0 0 0 0 0 0 0 0 0 0 0 0 0 0 0 0 0 0 /
0  0   0 0 0 0  0 0 0 0 0 0 0 0 0 0 0 0 0 0 0 0 0 0 0 0 0 0 0 0 0 0 0 0 0 0 0 /
0  0   0 0 0 0  0 0 0 0 0 0 0 0 0 0 0 0 0 0 0 0 0 0 0 0 0 0 0 0 0 0 0 0 0 0 0 /
```

Figure E-3. Input screen for model simulation of COM adsorption on hematite using inner-sphere complex formation for 1.48 mg/L COM (2.13 x 10^{-6} M), 74 ppm hematite (2.73 x 10^{-6} M), and 0.1 M total background electrolyte concentration as $NaClO_4$.

```
Adsorption of COM on hematite; calculations for 120 nm particles 74 ppm
Triple-Layer Model configuration: inner-sphere (o-plane) complexes
0.100  0   0.00  25.00 1.00E-5 1   100   /XMU   KEYMU ACTCOR  TEMP  EPS  NCASES  ITMAX
1     1     1     1     1     1          /IHYDRA  IINPUT  ICHARG  IPDIST  IPCENT IALLP
1     1     4     0     80000            /KEY   IADS   MODEL   IDIFOP   LIMADS
1.2   0.2   0     0.706  0   0   0   0   /C11  C21  C31  AREA1 C12  C22  C32  AREA2
117   50  86110  86105  86140  86130  86120  0  0  0  0  0  0  0  0  0  0  0  0 0/
2.5   9.5   0.5                          /line for pH stepping
174         -2.000    1.000E-1           /components          ClO4-
50          -4.000    0.0                /                    H+
5           -2.000    1.000E-1           /                    Na+
117         -8.000    2.130E-6           /                    COM
184         -8.000    2.730E-6           /                    SOH
180         -1        0.000              /                    PSIO
182         -1        0.000              /                    PSIB
183         -1.3      0.000              /                    PSID
0            0.000    0.000              /
2
2775        9.6       117   1    50    1    0     0   0   0   0   0   0   0/
2776        16.70     117   1    50    2    0     0   0   0   0   0   0   0/
2777        21.5      117   1    50    3    0     0   0   0   0   0   0   0/
86105       -10.3     184   1    50    -1   180   -1  0   0   0   0   0   0/
86110       6.7       184   1    50    1    180   1   0   0   0   0   0   0/
86115       -9.5      184   1    50    -1   180   -1  5   1   182 1   0   0/
86120       7.5       184   1    50    1    180   1   174 1   182 -1  0   0/
86130       29.1      184   1    50    3    117   1     0 0   0   0   0   0/
86131       24.6      184   1    50    2    117   1   180 -1  0   0   0   0/
86132       19.2      184   1    50    1    117   1   180 -2  0   0   0   0/
0           0         0     0    0     0    0     0   0   0   0   0   0   0/
3                                                                         /
50        4.00  0 0 0 0 0 0 0 0 0 0 0 0 0 0 0 0 0 0 0 0 0 0 0 0 0 0 0 0 0 0 0 /
0         0.00  0 0 0 0 0 0 0 0 0 0 0 0 0 0 0 0 0 0 0 0 0 0 0 0 0 0 0 0 0 0 0 /
6                                                                         /
180       0.00  0 0 0 0 0 0 0 0 0 0 0 0 0 0 0 0 0 0 0 0 0 0 0 0 0 0 0 0 0 0 0 /
182       0.00  0 0 0 0 0 0 0 0 0 0 0 0 0 0 0 0 0 0 0 0 0 0 0 0 0 0 0 0 0 0 0 /
183       0.00  0 0 0 0 0 0 0 0 0 0 0 0 0 0 0 0 0 0 0 0 0 0 0 0 0 0 0 0 0 0 0 /
0  0   0 0 0 0  0 0 0 0 0 0 0 0 0 0 0 0 0 0 0 0 0 0 0 0 0 0 0 0 0 0 0 0 0 0 0 /
0  0   0 0 0 0  0 0 0 0 0 0 0 0 0 0 0 0 0 0 0 0 0 0 0 0 0 0 0 0 0 0 0 0 0 0 0 /
```

Figure E-4. Input screen for model simulation of Th(IV) complexation with COM for 1.48 mg/L COM (2.13×10^{-6} M), 4×10^{-15} M Th(IV), and 0.01 M total background electrolyte concentration as $NaClO_4$.

```
Complexation of Th(IV) with COM
HYDRAQL solution complexation model:
0.010  0   0.00  25.00 1.00E-5 1   100   /XMU   KEYMU ACTCOR  TEMP  EPS  NCASES  ITMAX
1    1    1    1    1    1               /IHYDRA  IINPUT  ICHARG  IPDIST  IPCENT IALLP
1    0    0    0    80000                /KEY   IADS   MODEL   IDIFOP   LIMADS
0    0    0    0   0   0   0   0         /C11  C21  C31  AREA1  C12  C22  C32  AREA2
31   50  2778 0   0   0   0   0   0   0   0   0   0   0   0   0   0   0   0/
2.5   9.5   0.5                          /line for pH stepping
174          -2.000     1.000E-2         /components         ClO4-
117          -8.000     2.130E-6         /                   COM
50           -4.000     0.0              /                   H+
5            -2.000     1.000E-2         /                   Na+
31           -18.000    4.000E-15        /                   SOH
0             0.000     0.000            /
2
2775        9.6        117   1   50    1    0     0   0   0   0   0   0   0/
2776        16.70      117   1   50    2    0     0   0   0   0   0   0   0/
2777        21.5       117   1   50    3    0     0   0   0   0   0   0   0/
2778        25.5       117   1   31    1    50    2   0   0   0   0   0   0/
12090       -3.22      31    1   50    -1   0     0   0   0   0   0   0   0/
38011       -6.94      31    1   50    -2   0     0   0   0   0   0   0   0/
38012       -11.7      31    1   50    -3   0     0   0   0   0   0   0   0/
38013       -15.87     31    1   50    -4   0     0   0   0   0   0   0   0/
0           0          0     0   0     0    0     0   0   0   0   0   0   0/
3                                                                          /
50         4.00  0 0 0 0 0 0 0 0 0 0 0 0 0 0 0 0 0 0 0 0 0 0 0 0 0 0 0 0 0 0 0 /
0          0.00  0 0 0 0 0 0 0 0 0 0 0 0 0 0 0 0 0 0 0 0 0 0 0 0 0 0 0 0 0 0 0 /
0  0   0 0 0 0   0 0 0 0 0 0 0 0 0 0 0 0 0 0 0 0 0 0 0 0 0 0 0 0 0 0 0 0 0 0 0 /
```

Figure E-5. Input screen for model simulation of Th(IV) adsorption on hematite in the presence of COM for 4 x 10^{-15} M Th(IV), 1.48 mg/L COM (2.13 x 10^{-6} M), 74 ppm hematite (2.73 x 10^{-6} M), and 0.01 M total background electrolyte concentration as $NaClO_4$.

```
Ternary system - adsorption of Th(IV) on hematite; calculations for 120 nm particles 74 ppm
Triple-Layer Model configuration: inner-sphere (o-plane) complexes
0.0100 0   0.00  25.00 1.00E-5 1   100   /XMU   KEYMU ACTCOR  TEMP   EPS  NCASES  ITMAX
1   1   1   1   1   1                    /IHYDRA  IINPUT ICHARG  IPDIST  IPCENT IALLP
1   1   4   0   80000                    /KEY   IADS   MODEL   IDIFOP   LIMADS
1.2  0.2  0   0.706  0  0  0  0          /C11  C21  C31  AREA1 C12  C22  C32  AREA2
31  50  86110  86105  86140  86130  86120  0  0  0  0  0  0  0  0  0  0  0  0  0/
2.0   10.0   0.1                         /line for pH stepping
174         -2.000    1.000E-2           /components          ClO4-
50          -4.000    0.0                /                    H+
5           -2.000    1.000E-2           /                    Na+
31          -18.000   4.000E-15          /                    Th+4
117         -8.000    2.130E-6           /                    COM
184         -6.000    2.73100E-6         /                    SOH
180         -1        0.000              /                    PSIO
182         -1        0.000              /                    PSIB
183         -1.3      0.000              /                    PSID
0            0.000    0.000              /
2
12090       -3.22     31   1   50   -1   0     0   0   0   0   0   0   0/
38011       -6.94     31   1   50   -2   0     0   0   0   0   0   0   0/
38012       -11.7     31   1   50   -3   0     0   0   0   0   0   0   0/
38013       -15.87    31   1   50   -4   0     0   0   0   0   0   0   0/
2775         9.6      117  1   50   1    0     0   0   0   0   0   0   0/
2776        16.70     117  1   50   2    0     0   0   0   0   0   0   0/
2777        21.5      117  1   50   3    0     0   0   0   0   0   0   0/
2778        25.5      117  1   31   1    50    2   0   0   0   0   0   0/
86105       -10.3     184  1   50   -1   180   -1  0   0   0   0   0   0/
86110        6.7      184  1   50   1    180   1   0   0   0   0   0   0/
86115       -9.5      184  1   50   -1   180   -1  5   1   182 1   0   0/
86120        7.5      184  1   50   1    180   1   174 1   182 -1  0   0/
86130       17.3      184  1   50   -1   31    1   180 3   0   0   0   0/
86131       29.1      184  1   50   3    117   1     0 0   0   0   0   0/
86132       24.6      184  1   50   2    117   1   180 -1  0   0   0   0/
86133       19.2      184  1   50   1    117   1   180 -2  0   0   0   0/
0            0        0    0   0    0    0     0   0   0   0   0   0   0/
3                                                                       /
50         4.00   0 0 0 0 0 0 0 0 0 0 0 0 0 0 0 0 0 0 0 0 0 0 0 0 0 0 0 0 0 0 0 /
0          0.00   0 0 0 0 0 0 0 0 0 0 0 0 0 0 0 0 0 0 0 0 0 0 0 0 0 0 0 0 0 0 0 /
6                                                                       /
180        0.00   0 0 0 0 0 0 0 0 0 0 0 0 0 0 0 0 0 0 0 0 0 0 0 0 0 0 0 0 0 0 0 /
182        0.00   0 0 0 0 0 0 0 0 0 0 0 0 0 0 0 0 0 0 0 0 0 0 0 0 0 0 0 0 0 0 0 /
183        0.00   0 0 0 0 0 0 0 0 0 0 0 0 0 0 0 0 0 0 0 0 0 0 0 0 0 0 0 0 0 0 0 /
0  0   0 0 0 0    0 0 0 0 0 0 0 0 0 0 0 0 0 0 0 0 0 0 0 0 0 0 0 0 0 0 0 0 0 0 0 /
0  0   0 0 0 0    0 0 0 0 0 0 0 0 0 0 0 0 0 0 0 0 0 0 0 0 0 0 0 0 0 0 0 0 0 0 0 /
```